Lawrence Berkeley National Laboratory

Recent Work

Title

PULSE SHAPING AND STANDARDIZING OF PHOT (MULTIPLIER SIGNALS FOR OPTIMUM TIME INFORMATION USING TUNNEL DIODES

Permalink

https://escholarship.org/uc/item/0gj0p0n0

Authors

Bjerke, Arthur E.
Kerns, Quentin A.
Nunamaker, Thomas A.

Publication Date

1961-08-30

eScholarship.org Powered by the California Digital Library
University of California

For publication in Nuclear Instruments

UCRL-9838 c.2 rpl.
Limited distribution

UNIVERSITY OF CALIFORNIA

Lawrence Radiation Laboratory
Berkeley, California

Contract No. W-7405-eng-48

RECEIVED
LAWRENCE
BERKELEY LABORATORY

AUG 21 1987

LIBRARY AND
DOCUMENTS SECTION

PULSE SHAPING AND STANDARDIZING OF PHOTOMULTIPLIER SIGNALS FOR OPTIMUM TIMING INFORMATION USING TUNNEL DIODES

Arthur E. Bjerke, Quentin A. Kerns, and Thomas A. Nunamaker

August 30, 1961

TWO-WEEK LOAN COPY

This is a Library Circulating Copy
which may be borrowed for two weeks.

REVIEW COPY

UCRL-9838 c.2 rpl.

DISCLAIMER

This document was prepared as an account of work sponsored by the United States Government. While this document is believed to contain correct information, neither the United States Government nor any agency thereof, nor the Regents of the University of California, nor any of their employees, makes any warranty, express or implied, or assumes any legal responsibility for the accuracy, completeness, or usefulness of any information, apparatus, product, or process disclosed, or represents that its use would not infringe privately owned rights. Reference herein to any specific commercial product, process, or service by its trade name, trademark, manufacturer, or otherwise, does not necessarily constitute or imply its endorsement, recommendation, or favoring by the United States Government or any agency thereof, or the Regents of the University of California. The views and opinions of authors expressed herein do not necessarily state or reflect those of the United States Government or any agency thereof or the Regents of the University of California.

PULSE SHAPING AND STANDARDIZING OF PHOTOMULTIPLIER SIGNALS FOR OPTIMUM TIMING INFORMATION USING TUNNEL DIODES

Arthur E. Bjerke, Quentin A. Kerns, and Thomas A. Nunamaker

Lawrence Radiation Laboratory
University of California
Berkeley, California

August 30, 1961

ABSTRACT

Accurate timing signals have been derived from fast photomultiplier pulses by differentiating the photomultiplier pulse in order to produce a zero-crossing signal whose time of zero crossing is fixed over a large dynamic range of light level. Detection of the zero-crossing point is accomplished with a balanced-bridge tunnel-diode discriminator, which produces a standardized output pulse of 100-mv amplitude, and a half-width of 4 nsec. A balanced bridge is used to prevent the zero-crossing signal from appearing at the output.

For a twenty-to-one range of photomultiplier-input light level, the time shift of the output pulse may be as low as 0.5 nsec with a change in the output amplitude of less than a factor of two. When this discriminator is used with a 14-stage photomultiplier, the sensitivity is great enough to allow direct operation from single photo-electrons.

The above numbers are an indication of what one can obtain with the tunnel diode and transistor combination chosen at the time of the original development almost two years ago. Since that time, particularly in the tunnel-diode field, numerous improved devices have become available. We are currently evaluating these in zero-crossing circuits.

The zero-crossing photomultiplier pulse has been generated in two ways. The first method uses an overdamped LC-tuned circuit built into the base of a 6810-A photomultiplier. Here the time of zero crossing is controlled by the frequency of the LC-tuned circuit. The decay time of the scintillation plastic used and the rise time of the photomultiplier determine what this zero-crossing time should be. A clipping stub has also been used to produce the zero crossing remotely from the photomultiplier. By this method, one can control the zero-crossing time by both the length and impedance of the clipping stub.

PULSE SHAPING AND STANDARDIZING OF PHOTOMULTIPLIER SIGNALS FOR OPTIMUM TIMING INFORMATION USING TUNNEL DIODES*

Arthur E. Bjerke, Quentin A. Kerns, and Thomas A. Nunamaker

Lawrence Radiation Laboratory
University of California
Berkeley, California

August 30, 1961

THE PROBLEM

As the need for better timing resolution of nuclear experiments increases, the old problem of extracting the best possible timing information from the nuclear scintillations becomes increasingly important. The problem is complicated by the statistical nature of both the scintillation plastic and the photomultiplier as well as the large dynamic range of scintillation light encountered and the slow rise time of the photomultiplier output pulses. The best one can hope to do with an electronic circuit is to extract all the timing information contained in the output pulse of the photomultiplier, and supply this information in a useful form to other circuits with no dead time.

For timing application, a useful form for this output pulse might be a digital type of pulse having the same shape and amplitude regardless of the photomultiplier pulse amplitude, for this at once relaxes the large dynamic range requirements of subsequent electronics.

GENERAL THEORY OF OPERATION

One attempts to extract the best timing information possible from the photomultiplier pulse by using a large portion of the pulse. It is not desirable to use the whole pulse, because the tail of the pulse is distorted by the photomultiplier, nor is it desirable to use only the first electron arriving at the anode, since this ignores the timing information contained in the rest

of the pulse. By using a zero-crossing method, one can use a large portion of the photomultiplier pulse while ignoring its tail, thus extracting a large amount of the available timing information. Under conditions involving a weak scintillation light, however, the dominant problem is still photomultiplier and scintillation statistics.

A zero-crossing pulse that has a reasonably fixed crossing time maybe produced by differentiating the photomultiplier pulse with a time constant consistent with the photomultiplier rise time and scintillation plastic decay time. Both a clipping-stub method and a critically-damped LC tank-circuit method have been used for this differentiation. With the clipping-stub method, the point of zero crossing is controlled by both the length and impedance of the clipping stub. In the LC tank method, the zero-crossing point is controlled by the resonant frequency of the tank circuit.

A tunnel-diode discriminator has been used to detect the time of zero crossing. This circuit consists of a balanced bridge with a tunnel diode in one leg of the bridge. The tunnel diode regenerates at the point of zero crossing, producing an output at the phantom ground point of the bridge. Because the timing information of the photomultiplier is contained in the leading edge of the tunnel-diode signal, this signal is differentiated, and the back swing clipped off. The resulting output pulse contains the timing information of the original photomultiplier pulse without its large amplitude variation.

CIRCUIT EVALUATION

There are essentially two circuit problems to resolve here. The first is to find a suitable means of producing a zero-crossing signal from the photomultiplier pulse; the second, to find a circuit for detecting this zero crossing.

Tunnel diodes are quite suitable for detection because they have fast switching times, can tolerate large signals in either direction without damage or hysteresis, and exhibit good stability of their characteristic. If the tunnel diode exhibits hysteresis--that is, if the forward characteristic depends upon how hard the diode is driven in the backward direction--the present circuits will be much less effective. Fortunately, however, the regeneration threshold is not detectably affected by the backward pulse which first appears in a zero-crossing circuit.

The simplest circuit is a shunt tunnel diode driven directly by the source. Unfortunately, when operated over a large dynamic range of input amplitude the output also has a large amplitude variation. This is because the positive resistance and inductance of the tunnel diode are not zero and thus allow feedthrough of the driving pulse. This feedthrough may be reduced by differentiating the output of the tunnel diode in cases where the switching time of the tunnel diode is fast in relation to the rise time of the photomultiplier, but at present this rise time difference is not great enough to give a suitable reduction in feedthrough. The sensitivity of this shunt circuit may be improved by the addition of an impedance-matching transformer between the driving source and tunnel diode. (This has been referred to as the Fitch circuit). The feedthrough problem may be reduced considerably by employing a balanced bridge arrangement in which the tunnel diode is placed in one leg of the bridge, and the bridge is adjusted to balance out the positive resistance of the tunnel diode. If a signal is taken from the phantom ground point of the bridge there will be an output only when the tunnel diode regenerates over its nonlinear characteristic.

TUNED LC ZERO CROSSING ON 6810-A BASE

A special tunnel-diode discriminator[2,3] has been built into a socket

structure for a 6810-A photomultiplier in order to obtain highest discriminator sensitivity (i. e., lowest photomultiplier gain and noise) while avoiding the problem of multiple reflections encountered when a tunnel diode and photomultiplier are connected together by a long transmission line (Fig. 1). The discriminator consists of a balanced bridge with a tunnel diode in one leg of the bridge. A photomultiplier pulse is applied to the bridge through a slightly overdamped 80-Mc LC circuit and fires the discriminator at the first point of zero-crossing of the damped signal. The resonant frequency of the LC zero-crossing circuit was chosen to be compatible with the rise time of the photomultiplier and the decay time of the scintillation plastic combination. Time definition of the original photomultiplier pulse is maintained to better than 1/2 nsec over a 20 to 1 dynamic range by the discriminator output pulse. The input charge sensitivity can be made as low as 4 μμcoulombs, that is, 2.5×10^7 electrons. In terms of the 6810-A gain this means that the over-all photomultiplier discriminator sensitivity is more than sufficient to allow operation from single photoelectrons at the cathode of the photomultiplier. The output pulse of the discriminator varies in amplitude by about two to one when the discriminator is operated over its useful dynamic range of twenty to one. The unit-to-unit amplitude ranges from 40 to 100 mv without selection of tunnel diodes and transistors. This variation may be reduced considerably by selection. Threshold stability referred to the "tube signal" output (Fig. 1) is 240 μv/°C without compensation and may be reduced to 10 μv/°C over a temperature range of -3 to 35°C.

Though the unit was designed specifically for a 6810-A photomultiplier, the 7264, 7265, CL-1090, CL-1019, and the CL-1004 types also plug directly into the socket. For noncritical applications, sockets are interchangeable, however, to obtain the best timing or collection efficiency, one must adjust the focus-electrode voltage.

Threshold adjustment for the discriminator is remotely located. Two signals are available from the unit on separate 125-ohm cables: the discriminator output signal and a zero-crossing "tube signal" (Fig. 1). The latter is proportional to the charge delivered to the photomultiplier anode and has an amplitude of about 10% of the direct anode pulse when delivered into 125 ohms impedance. This pulse may be fed to pulse-height-analyzing equipment or used for monitoring.

The discriminator is mounted directly behind the tube socket on a circular printed-circuit board supported by a brass rod that connects the socket to the rear base plate (see Figs. 2 and 3). Two similar printed-circuit boards directly behind the discriminator contain the high-voltage divider resistors which are wired to the socket by means of two ribbon Teflon-insulated cables. Since the whole socket assembly is removable from the rear, one need not unsolder the signal and high-voltage connections when removing the socket from its housing. An experimental housing has been made which consists of a spun aluminum shell and end cap. These two housings are shown in Fig. 4.

OPERATION CHARACTERISTICS

A typical slewing characteristic of the circuit is shown in Fig. 5; the "slewing characteristic" of a trigger circuit is the time shift of the output pulse as a function of the input pulse amplitude. The characteristic is U-shaped, with the discriminator triggering late for very small and very large photomultiplier signals, the curve being essentially flat in the center. For small photomultiplier signals there is slewing until the pulse is about three times as large as threshold. At that point time shifts become small (i. e., small but finite, since the circuit is biased not at zero, but slightly away from zero)

for increasing photomultiplier signals until space-charge saturation of the photomultiplier starts setting in. When this occurs, the pulse shape of the photomultiplier begins changing, forcing the discriminator to fire late. In order to forestall this effect, a tapered high-voltage divider is used which places higher voltages across the later sections of the photomultiplier, thus allowing higher current levels before space-charge saturation sets in. Figure 6 shows the amplitude linearity of the zero-crossing "tube signal" as a function of the number of photoelectrons from the cathode for photomultiplier gains of 3×10^5, 3×10^6, and 3×10^7.

Once one states the minimum threshold at which the discriminator may be set, the maximum possible dynamic range may be interpreted as the linear region between threshold and saturation. The minimum discriminator threshold is about 5 mv of peak zero-crossing "tube signal", thus establishing the maximum dynamic range of about one-hundred to one. Since the saturation portion of these curves is fixed by the characteristic of the photomultiplier, the dynamic range can only be extended by lowering the discriminator threshold. There are two factors that limit this threshold. The first is the problem of regeneration. If the discriminator threshold is lowered, eventually a relaxation oscillation occurs at an equivalent threshold of a few millivolts. This minimum threshold is determined by the circuit associated with the tunnel diode, and the amplitude of the tunnel-diode signal. That is, the tunnel diode having large voltage swings (gallium arsenide) will go into relaxation oscillation at a higher threshold than a diode having lower voltage swings (germanium), because the larger signal forces oscillation sooner. Thus, since the germanium tunnel diode has the smaller swing it will have a larger dynamic range. The use of gallium arsenide has been discouraged also by its reported long-term instability.

The second factor that limits the threshold is the worsening of the initial slewing characteristics (Fig. 5) as the threshold is lowered, i.e., the slope of the slewing characteristics near threshold becomes less as the threshold is lowered. This is due to the response of the discriminator to overdrive signal in excess of threshold. For example, if the discriminator threshold is 10 mv, then a signal of 20 mv represents a factor-of-two overdrive or 10-mv overdriving signal. However, if the threshold is set at 20 mv, then a factor of two of overdrive represents 20 mv of overdriving signal. Thus the effective overdriving signal becomes greater as the discriminator threshold is made less sensitive, resulting in the better slewing characteristic near threshold.

For very large photomultiplier signals (100 times threshold), the output pulse of the discriminator will grow about 200% over its threshold value for a bridge unbalance of 2%. This is shown in Fig. 5 along with the slewing characteristics. Recovery time of the discriminator is of the order of 25 nsec, and under the most favorable conditions of a small pulse followed by a large pulse, the unit will accept pulses 10 nsec apart. As the amplitude of the second pulse is increased, the recovery delay decreases, because the second pulse begins to overpower the back swing of the first pulse. The delayed firing action of the zero-crossing circuit allows a small initial pulse to be completely overpowered by a larger second pulse if the second pulse arrives 10 to 15 nsec after the first pulse. This results in the second pulse producing an output while the first pulse produces no output.

A typical discriminator output-pulse waveshape is shown in Fig. 7. This pulse has a triangular shape with a base width of 9 nsec.

The zero-crossing "tube signal" may be used to monitor the operation of the photomultiplier, since this signal is proportional to the peak ansde current. Figure 8 shows waveshapes of the tube signal over a range of amplitudes. A test signal may be injected at this point to set the discriminator threshold to any desired peak anode-current level.

GENERALIZED TUNED LC ZERO-CROSSING DESCRIPTION

The response of the tuned LC zero-crossing network to an applied pulse i(t) is

$$v(t) = i(t)\, Z, \tag{1}$$

where i(t) is the driving function and Z is the network function. For an idealized zero-crossing detector, the zero-crossing time, t_z, is defined by

$$v(t_z) = 0. \tag{2}$$

Thus at the point of zero crossing, Eq. 1 reduces to

$$0 = i(t_z)\, Z. \tag{3}$$

Once we have the input function i(t), we can find t_z from Eq. 3. This has been done in Appendix A under the idealized condition of i(t) being a generalized triangular current pulse

$$i(t) = K_1 t - (K_1 + K_2)(t-t_a)\, \mu(t-t_a). \tag{4}$$

In this latter expression, t_a is the time of the peak of the input triangular pulse, K_1 is the slope of the initial portion of the input pulse, and $-K_2$ is the slope of the trailing portion of the input pulse. The unit jump function is $\mu(t-t_a)$, where

$$\left.\begin{aligned}\mu(t-t_a) &= 0\\ &= 1\end{aligned}\right\} \qquad \begin{aligned}0 &\leqslant t \leqslant t_a\\ t_a &\leqslant t.\end{aligned} \tag{5}$$

The response of the zero-crossing circuit to this input is

$$v(t)=L\left\{K_1[1-(1+t_z')e^{-t_z'}] - (K_1+K_2)[1-(1+t_z'-t_a')\,e^{-(t_z'-t_a')}]\,\mu(t_z-t_a)\right\}. \tag{6}$$

In this expression t_z and t_a have been normalized with respect to the frequency of the zero-crossing circuit:

$$t_z' = \frac{t_z}{\sqrt{LG}} \tag{7}$$

$$t_a' = \frac{t_a}{\sqrt{LC}}. \tag{8}$$

Equation (6) applies for

$$t_a \leqslant t_z \leqslant t_a\left(\frac{K_1}{K_2}+1\right). \tag{9}$$

Applying the zero-crossing condition to Eq. (6), we have an implicit expression for t_z' containing two independent variables (t_a' and K_1/K_2). Thus we can plot the solution for t_z' as a series of constant t_z' curves on the (t_a', K_1/K_2) plane. Such a solution is shown in Fig. 19 of Appendix A, and is useful in predicting timing shifts with changes in pulse shape. As the frequency of the zero-crossing circuit is varied, t_z moves along constant K_1/K_2 contours on this plot.

If for the sensitivity of the circuit, we take the rate of change of current in the load conductance G at the zero-crossing point, we have from Eq. (A21) of Appendix A,

$$\frac{di_G(t_z)}{dt} = \frac{4Q_T}{t_a^2\left(\frac{K_1}{K_2}+1\right)}\, e^{-t'_z}\left[t'_z - \left(1+\frac{K_2}{K_1}\right)(t'_z - t'_a)\, e^{t'_a}\right]. \qquad (10)$$

Here the only new term is Q_T, the total charge contained in the input pulse. Evaluating this expression for a triangular pulse of 5-nsec rise, 10-nsec fall, and a total charge of 1 μμcoul, we have for an 80-Mc tank frequency (in μa/nsec).

$$\frac{di_G(t_z)}{dt} \simeq 17. \qquad (11)$$

We may now use this expression to estimate the timing uncertainty due to tunnel-diode noise. The noise current of a 1N2941 tunnel diode with 5-ma peak current is of the order of 2 μa, and thus there will be a timing uncertainty of about 120 psec due to tunnel-diode noise for an input charge of 1 μμcoul.

CIRCUIT DESCRIPTION

Photomultiplier-signal current flows through the two series primary windings (P_1 and P_2 of Fig. 1) of transformer T_1 (see Appendix B).[4] Two windings are used to allow placement of ac ground at a favorable point between the anode and D14. Placement is determined by capacity measurements between electrodes as indicated by the dotted lines in Fig. 1. As can be seen from the interelectrode capacitance distribution, ground should be approximately one third along the primary from D14 to the anode.

The shunt inductance of the transformer plus the capacity appearing between the anode and D14 forms an 80-Mc tuned circuit which is overdamped by 275 ohms to produced the zero-crossing pulse. The resonant frequency of this tuned circuit is chosen by considering the rise time of the photomultiplier and the decay time of the scintillation plastic used.

The zero-crossing pulse appears as a push-pull signal on secondary S_1 of T_1. This secondary S_1 along with the tunnel diode CR1 and the two selected resistors R4 and R12 form a bridge which is balanced to about 2% when the tunnel diode is biased a few millivolts below the regenerative point. The series inductance L_1 and L_2 in the transformer leads buffers the tunnel diode from the tuned circuit, since energy flow from the regenerating tunnel diode to the tuned circuit and back again may cause a second regeneration. Resistors R_1 and R_2 are of low value to permit the tunnel diode only one stable state. With a sufficiently large photomultiplier signal, the tunnel diode regenerates, causing a positive signal to appear at the output of the bridge. The pulse width is dependent upon the photomultiplier signal amplitude, and examination shows the front edge of this pulse to be time-stable. In order to remove the width variation[5] and utilize the front edge, the signal is differentiated by a 50-$\mu\mu$f capacitor C_1 and the input impedance of the 2N1143

grounded-base transistor amplifier. Because the transistor is biased with a low standing current (0.1 ma), only the positive portion of the differentiated pulse is passed. The transistor output is available on a 125-ohm coaxial line whose center conductor also serves to carry bias current to the tunnel diode. Threshold adjustment is thus made remotely from the photomultiplier.

A zero-crossing monitor signal is taken from the transformer secondary S_2 and is available on a 125-ohm line. Since the secondary S_2 has an input impedance of about 30 ohms, the 100-ohm series resistor R_3 reverse-terminates the monitor line. Direct-current power for the transistor is taken from the phototube high-voltage supply.

MECHANICAL DESIGN

Because the 6810-A tube base is designed to have the tunnel-diode discriminator as an integral part of the base, it has been necessary to design the whole socket structure. The discriminator is mounted as close to the socket as possible on a circular printed-circuit board (Figs. 2 and 3), and the high-voltage resistive divider is placed behind the discriminator wafer. The high-voltage divider resistors are mounted in a doughnut fashion between two circular printed-circuit boards, eyelets being used in the printed-circuit boards for protection against repeated soldering. Deposited carbon resistors have been used in some dividers because of their good stability.[6] These resistors are now fairly inexpensive.

The printed-circuit boards are held together by means of a brass rod which is secured to the socket with a glass-Epoxy disk (Figs. 2 and 3). The spacing between boards is controlled with insulating tubes placed over the brass rod, and the entire assembly is held together in compression with a nut at the end of the rod (see Fig. 3). The base plate containing all the cable

connectors is secured to the end of the rod, forming a rigid mechanical structure.

It is possible to disassemble the base and add or remove the discriminator circuit board without unsoldering the high-voltage divider. A complete base subassembly (Fig. 4) may be removed from its housing, thus allowing easy replacement under field conditions.

The high-voltage divider resistors are connected to the socket with two Teflon-insulated ribbon cables.[7] These ribbon cables are placed on opposite sides of the printed-circuit boards, with one cable picking up all connections from the lower printed-circuit board and the second cable all connections from the upper printed-circuit board. It has been possible to arrange the wires in each cable so that there is a nearly uniform voltage gradient across the cables, thus reducing the dielectric stress from wire to wire.

The tube base may be mounted in a standard UCLRL 6810 housing or an experimental housing which consists of a spun aluminum shell (see Fig. 4). Spinning offers an inexpensive method of producing the housing and has the advantage of a circular end plate, thus removing the problem of keying the socket to both the phototube as well as the housing. The socket is secured to the housing with latches accessible from the rear, thus making possible removal of the socket when the sides of the housing are inaccessible.

CLIPPING-STUB ZERO-CROSSING CIRCUIT

The circuit shown in Fig. 9 differs from the previous one only in that the zero-crossing signal is produced by means of a clipping stub rather than an overdamped LC tank circuit. The other major difference is that the discriminator and photomultiplier are connected through a transmission line as opposed to being built directly on the base of the photomultiplier.

Signal flow in the clipping stub is represented in Fig. 10. The input $mf(t)$, where m is an amplitude constant, is split into two paths--the direct path and a delayed path having gain A and delay τ. These two functions are then added to produce the output $z(t)$, where

$$z(t) = mf(t) + Amf(t-\tau). \tag{12}$$

For an idealized zero-crossing detector, the time of zero crossing is defined as

$$z(t_z) = 0. \tag{13}$$

At the point of zero crossing, Eq. (12) reduces to

$$0 = mf(t_z) + Amf(t_z - \tau). \tag{14}$$

The input amplitude m drops out, leaving

$$f(t_z) = - Af(t_z - \tau) \tag{15}$$

It is now apparent (Fig. 11) that the zero-crossing time t_z is determined by only two points of the original function f; thus establishing t_z as the time when the ratio of these two points, $f(t_z)$ and $f(t_z - \tau)$ is a specified constant, namely A. Solutions for the zero-crossing time for a generalized triangular input are shown in Appendix A. For these triangular input pulses, t_z and $(t_z - \tau)$ may be placed anywhere along the original pulse by suitable choices of A and τ.

The sensitivity of clipping-stub circuit has been found in Appendix A for the case in which the input is a triangular pulse and the clipping stub is placed at the photomultiplier. Under these conditions the rate of change of

current in the load at the zero-crossing time t_z is

$$\frac{di_L(t_z)}{dt} = \frac{2Q_T}{t_a^2\left(1+\frac{K_1}{K_2}\right)}\left(A - \frac{K_2}{K_1}\right)\left(1 + \frac{A}{2}\right). \tag{16}$$

For a triangular input pulse having a 5-nsec rise, 10-nsec fall (that is $K_1/K_2 = 2$); a total charge Q_T of 1 μμcoul; and critical damping (that is $A = -1$, with no multiple reflections in the clipping stub); we have

$$\frac{di_L(t_z)}{dt} = 20\ \mu a/nsec. \tag{17}$$

For the clipping-stub circuit there are certain restrictions on A, but not on τ. For the clipping arrangement used to date (Fig. 12) A may be expressed as

$$A = -\frac{V_N}{V_P} \tag{18a}$$

and

$$A = -\frac{1}{\frac{1}{2} + \frac{Z_C}{Z_O}} \tag{18b}$$

where V_N is the inverted and delayed pulse, and V_P is the directly transmitted pulse in Fig. 12. The over-all gain of the clipping arrangement is

$$\frac{V_N}{V_S} = \frac{1}{1 + \frac{1}{4}\ \frac{Z_O}{Z_C} + \frac{Z_C}{Z_O}}. \tag{19}$$

If we take the limit of these last two expressions as the clipping-stub impedance Z_C approaches zero, we have

$$\lim_{Z_C \to 0} A \to -2 \tag{20}$$

and

$$\lim_{Z_C \to 0} \frac{V_N}{V_S} \to 0. \tag{21}$$

In this limit the over-all gain goes to zero as A approaches its minimum valse of minus two. As there must be a useable over-all gain, Z_C must be finite; consequently we have

$$|A| < 2. \tag{22}$$

Figure 12 is a graphical representation of Eq. (18) and (19) and may be used to compare A with the over-all gain as a function of Z_C.

For the values of A and τ used to date, the zero-crossing time t_z has been later than the peak of the original photomultiplier pulse. We observe that the later is t_z, the more severe is the time slewing in the early region of photomultiplier saturation. This effect is due to the change in photomultiplier pulse shape and may be reduced slightly by adjusting A and τ to make t_z come closer to the peak of the photomultiplier pulse.

OPERATING CHARACTERISTICS

The slewing characteristic for a clipping-stub circuit and 7046 photomultiplier is shown in Fig. 13 and is very similar to the tuned circuit and 6810-A photomultiplier slewing characteristic in Fig. 5. The significant difference is in the region of large light levels, where the photomultiplier is entering space-charge saturation. At this point, the time shifts are greater for the tuned LC circuit than the clipping-stub circuit. This is due in part to the earlier zero crossing obtained with the clipping-stub circuit and in part to the different photomultiplier and divider tapers used. The output pulse has an amplitude variation of 40% when operated over its useful dynamic range.

Threshold stability has been obtained over a 2-month period on 96 of these units. These data indicate an instability of about 10% (17 mv) over this period and are shown in Fig. 14. Figure 14 shows the change (a) during the first month and (b) during two months.

The uncompensated temperature coefficient of this unit is -0.1 mv/°C. Figure 15 shows 100 of these units mounted in a large nuclear experiment. Figure 16 shows a single-channel circuit built into a plug-in box.

COMPARISON OF ZERO-CROSSING METHODS

The major difference between these two zero-crossing methods is the relation of the zero-crossing pulse to the original photomultiplier pulse. The clipping stub simply compares two points on the photomultiplier pulse, the only smoothing being the finite bandwidth of the tunnel diode and its associated bridge circuit. With the tuned LC circuit the bandwidth of the circuit is intentionally lowered; thus there is more smoothing of the original photomultiplier pulse.

The sensitivity of the tuned-LC and clipping-stub circuits are nearly identical, however the tuned-LC circuit may use the stray capacity of the photomultiplier as an integral part of its circuit, thus affording some improvement in sensitivity. Also, since the tuned-LC circuit inductance is built on a Ferroxplana core, the necessary transformation to the tunnel-diode impedance level is obtained simply by additional windings on the same core. On the other hand, the clipping stub presents no direct means of impedance transformation.

If either zero-crossing network is located remotely from the photomultiplier by a transmission line, there is a loss of sensitivity of a factor of two due to the reverse termination of the transmission line. In this case it is not possible to use the stray capacity of the photomultiplier as part of the tuned LC circuit.

OPERATING HISTORY

Over 90 of the tuned LC units have been built and successfully operated in various counting experiments during the past three months. Seventy-five units were operated in a single experiment with a high degree of reliability. Long-term threshold stability has been measured on 100 of the clipping-stub models while operating in a nuclear experiment and was within 10% over a 2-month period. Since the tune LC discriminator circuit is essentially the same, the threshold stability should be similar to that of the clipping-stub unit. The effect of large, stray, pulsed magnetic fields near the Bevatron has been observed to produce a 1% change in threshold.

ACKNOWLEDGMENTS

We wish to thank Messrs. Fred A. Kirsten, George M. Sheldon, and Robert F. Reynolds for their contributions to the mechanical layout, as well as Messrs. Robert F. Tusting and Cordon R. Kerns for their work on the high-voltage divider design and photomultiplier data.

APPENDIXES

A. Zero-Crossing Analysis for an Idealized Triangular Current Pulse Input.

1. Tuned LC zero-crossing analysis

The input impedance of the tuned LC network (Fig. 17) in terms of the Laplace transformation is

$$Z_S = \frac{SL}{S^2\,LC + SLG + 1} . \tag{A1}$$

Figure 18 shows the triangular pulse that will be used. For the range of time from zero to $t_a[(K_1/K_2) + 1]$, the expression for this pulse is

$$i(t) = K_1 t - (K_1 + K_2)\,(t - t_a)\,\mu(t - t_a), \tag{A2}$$

where K_1 is the slope in the first interval ($t \leqslant t_a$), $-K_2$ is the slope in the second interval ($t_a \leqslant t \leqslant t_a[(K_1/K_2) + 1]$, t_a is the time of the peak of the pulse, and $\mu(t - t_a)$ is the unit step function translated in time and defined as

$$\begin{aligned} \mu(t - t_a) &= 0 \qquad \text{for} \quad 0 \leqslant t \leqslant t_a \\ &= 1 \qquad \text{for} \quad t_a \leqslant t. \end{aligned} \tag{A3}$$

The Laplace transform of Eq. (A2) is

$$I(S) = \frac{K_1}{S^2} - \frac{K_1 + K_2}{S^2}\, e^{-t_a S} . \tag{A4}$$

The voltage across the LC tank in terms of the Laplace transform is

$$V(S) = I(S)\, Z(S) \tag{A5}$$

Substituting Eq. (A1) and (A4) into (A5) gives

$$V_{(S)} = \left(\frac{K_1}{S^2} - \frac{K_1 + K_2}{S^2} \; e^{-t_a S} \right) \frac{SL}{S^2 LC + SLG + 1} . \tag{A6}$$

For the case of critical damping being considered here, we have

$$GZ_0 = 2, \tag{A7}$$

where

$$Z_0 = \sqrt{L/C} \; . \tag{A8}$$

Applying the critical-damping condition to Eq. (A6) gives

$$V_{(S)} = \left(\frac{K_1}{S^2} - \frac{K_1 + K_2}{S^2} \; e^{-t_a S} \right) \frac{S}{C\left(S + \frac{1}{\sqrt{LC}}\right)^2} . \tag{A9}$$

Equation (A9) may now be transformed back into the time domain

$$V(t) = L \left\{ K_1 \left[1 - (1+t') \, e^{-t'} \right] - (K_1 + K_2) \left[1 - (1 + t' - t_a') \, e^{-(t' - t_a')} \right] \mu(t - t_a) \right\}, \tag{A10}$$

where

$$t' = \frac{t}{\sqrt{LC}} \; , \tag{A11}$$

$$t_a' = \frac{t_a}{\sqrt{LC}} \; , \tag{A12}$$

and

$$0 \leq t \leq t_a \left[(K_1/K_2) + 1 \right] . \tag{A13}$$

The time of zero-crossing is defined by

$$V(t_z) = 0. \tag{A14}$$

Under this condition Eq. (A10) becomes

$$0 = 1 - (1+t_z')\, e^{-t_z'} - (1+ K_2/K_1)[1-(1+t_z' - t_a')\, e^{-(t_z' - t_a')}] \qquad (A15)$$

for $t_a \leq t_z \leq t_a [(K_1/K_2) + 1]$. As there are only two independent variables in Eq. (A15), we can plot a family of curves with constant t_z' on the $(K_1/K_2, t_a')$ plane. This is shown in Fig. 19.

To find the sensitivity, we evaluate the derivative of Eq. (10) at the zero-crossing time t_z:

$$\frac{dV(t_z)}{dt} = Z_0 K_1\, e^{-t_z'} \left\{ t_z' - (1+ K_2/K_1)(t_z' - t_a')\, e^{t_a'} \right\} \qquad (A16)$$

for $t_a \leq t_z \leq t_a [(K_1/K_2) + 1]$.

If we consider the load to consist of the critical damping conductance G, then we may rewrite Eq. (A16) in terms of the current in the load conductance

$$\frac{diG(t_z)}{dt} = 2K_1\, e^{-t_z'} \left\{ t_z' - (1+ K_2/K_1)(t_z' - t_a')\, e^{t_a'} \right\} \qquad (A17)$$

for $t_a \leq t_z \leq t_a [(K_1/K_2) + 1]$.

The constant K_1 is related to the total input charge Q_T and is found by integrating the triangular input, Eq. (A2):

$$Q_T = \int_0^{t_a(K_1/K_2+1)} i(t)\, dt \qquad (A18)$$

$$Q_T = \frac{K_1\, t_a^{\,2}}{2} (1 + K_1/K_2). \qquad (A19)$$

Rearranging, we have

$$K_1 = \frac{2\,Q_T}{t_a^2(1+K_1/K_2)}. \tag{A20}$$

Substituting Eq. (A20) into (A17) gives

$$\frac{di_G(t_z)}{dt} = \frac{4Q_T}{t_a^2(1+K_1/K_2)} e^{-t'_z}\left\{t'_z - (1+K_2/K_1)(t'_z - t'_a)\,e^{t'_a}\right\} \tag{A21}$$

for $t_a \leq t_z \leq t_a[(K_1/K_2)+1]$.

Let us evaluate this for a pulse with a 5-nsec rise, 10-nsec fall, a total charge of 1 μμcoul, and an 80-Mc tank frequency:

$$Q_T = 10^{-12}\ \text{coul}$$
$$t_a = 5\times 10^{-9}\ \text{sec}$$
$$K_1/K_2 = 2$$
$$\sqrt{LC} = 2\times 10^{-9}\ \text{sec}$$
$$t'_a = 2.5$$
$$t'_z = 4.7 \quad [\text{From Fig. 19 or Eq. (A15)}]$$

Putting these numbers into Eq. (22) gives

$$\frac{di_G(t_z)}{dt} \simeq 17\ \mu\text{a/nsec}. \tag{A22}$$

It is instructive to compare this with the noise current of a tunnel diode in-order to estimate the timing uncertainty. For a germanium tunnel diode with 5-ma peak current, the noise current is of the order of 1 or 2 μa; thus the timing uncertainty for this 1 μμcoul of input charge is on the order of a 100 psec.

2. Clipping-Stub Zero-Crossing Analysis

We consider here the same idealized triangular pulse as was used in Eq. (A2), as shown in Fig. 20. When we apply this pulse to the clipping-stub Eq. (12), and apply the zero-crossing condition, Eq. (13) we have

$$0 = K_1 t_z - (K_1 + K_2)(t_z - t_a)\,\mu(t_z - t_a) + A\left\{K_1(t_z - \tau)\,\mu(t_z-\tau) - (K_1+K_2)[t_z-(t_a+\tau)]\,\mu[t_z-(t_a+\tau)]\right\}, \tag{A23}$$

where $\tau \leqslant t_z \leqslant t_a\,[(K_1/K_2) + 1]$. As we are dealing with discontinuous functions it is necessary to consider each continuous region separately:

a. The first solution is for the interval $\tau \leqslant t_z \leqslant t_a$.

Solving Eq. (A23) for this region gives

$$t_z = \frac{A\tau}{1+A}, \tag{A24}$$

where $A < -1$. Since the zero-crossing occurs before the peak of the input, this is the special case of the input being a ramp function.

b. The next solution is for the interval $\tau \leqslant t_a \leqslant t_z \leqslant t_a + \tau$ or $t_a \leqslant \tau \leqslant t_z \leqslant t_a + \tau$. Again solving Eq. (A23), we have

$$t_z = \frac{A\tau\,\dfrac{K_1}{K_2} - t_a\left(\dfrac{K_1}{K_2} + 1\right)}{A\,\dfrac{K_1}{K_2} - 1}. \tag{A25}$$

c. The last interval is $t_a + \tau \leqslant t_z \leqslant t_a\,[(K_1/K_2 + 1)]$. From Eq. (A23) we have

$$t_z = t_a\,(K_1/K_2 + 1) + \frac{A}{1+A}\,\tau. \tag{A26}$$

The solutions for t_z are functions of four independent constants; therefore we must fix one and normalize with respect to another in order to plot constant t_z curves. These constant t_z solutions are shown in Fig. 21 for a fixed A of - 1.28, the value used for the clipping-stub circuit to date. Time is normalized with respect to τ, the total delay of the clipping stub; thus we have

$$t_z' = \frac{t_z}{\tau} \tag{A27}$$

and

$$t_a' = \frac{t_a}{\tau} \ . \tag{A28}$$

To find the maximum sensitivity of the clipping-stub circuit, we place the clipping stub at the photomultiplier. Thus we have the circuit of Fig. 22. The current in the load R is

$$i_L(t) = i(t)\ (1 + \frac{A}{2}) \ , \tag{A29}$$

where

$$A = - \frac{2}{1 + \frac{Z_C}{R_L}} \ . \tag{A30}$$

The partial derivative of Eq. (A29) is

$$\frac{\partial i_L(t)}{\partial t} = \frac{\partial i(t)}{\partial t}\ (1 + \frac{A}{2}). \tag{A31}$$

The derivative $\partial i(t)/\partial t$ of the input is

$$\frac{\partial i(t)}{\partial t} = K_1 A - K_2 \ , \tag{A32}$$

where the zero crossing is after the peak $t_a \leqslant \tau \leqslant t_z \leqslant t_a[(K_1/K_2) + 1]$ or $\tau \leqslant t_a \leqslant t_z \leqslant t_a\ [(K_1/K_2) + 1]$.

Combining Eqs. (A31) and (A32) gives

$$\frac{\partial i_L(t)}{\partial t} = (K_1 A - K_2)\left(1 + \frac{A}{2}\right). \tag{A33}$$

For the case of critical damping (that is, for no reflections in the clipping stub) we have $A = -1$. Substituting K_1 from Eq. (A20) gives

$$\frac{\partial i_L(t)}{\partial t} = -\frac{Q_T}{t_a^2}\frac{K_2}{K_1}. \tag{A34}$$

Evaluating Eq. (A34) for a pulse with a 5-nsec rise, 10-nsec fall, and a total charge of 1 μμcoul, we have (in μa/nsec)

$$\frac{\partial i_L(t)}{\partial t} \simeq 20. \tag{A35}$$

3. Comparison of sensitivity

It is possible to compare the sensitivities of the tuned-LC and clipping-stub circuits by taking the ratio of Eqs. (A21) and (A34):

$$D \triangleq \frac{\dfrac{\partial i_G(t)}{\partial t}}{\dfrac{\partial i_L(t)}{\partial t}} \tag{A36}$$

$$D = 4\, e^{-t_z'}\left\{\frac{t_z'}{1 + \dfrac{K_2}{K_1}} - (t_z' - t_a')\, e^{t_a'}\right\}. \tag{A37}$$

This D ratio is plotted in Fig. 23. Here we see that for small K_1/K_2 (that is, for pulses with fall times comparable with their rise time) the tuned LC circuit is slightly more sensitive, while for large K_1/K_2 (that is, pulses with relative long tails) the clipping-stub circuit is slightly more sensitive.

B. Transformer T_1.

The ferrite-cored transformer designed for direct phototube mounting of the tunnel-diode discriminator is shown in Fig. 24. It is mounted at the phototube socket. The zero-crossing pulse is produced by the parallel combination of the phototube output capacitances, the transformer shunt inductance, and damping resistors.

Construction

Coils:

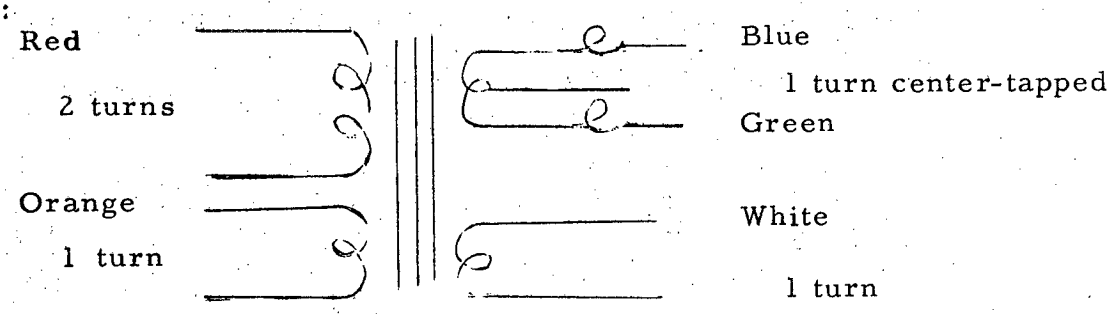

Core: Ferroxcube Corporation of America
2P64-237 1Z2

Wire lengths:			
	Red	4-1/4 in.	No. 22 Teflon-insulated wire
	Orange	2-1/4 in.	
	Blue	3-1/8 in.	
	Green	3-1/8 in.	
	White	3-3/4 in.	No. 30 Teflon-insulated wire

Tektronix LC-meter measurements

Inductance (nh)	Other windings open	Other windings shorted
Primary (red and orange in series):	720	250
Center-tapped secondary: (series inductance in each of blue and green leads is 35 nh)	150	100
White-wire secondary:	100	30

Capacitance (pf)

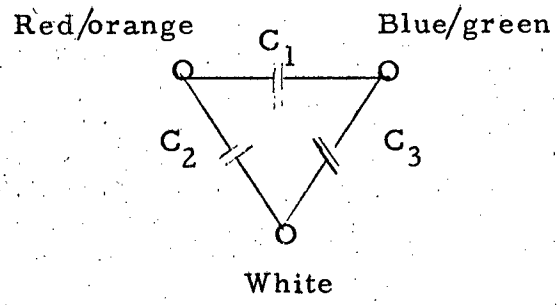

$C_1 = 2.9$
$C_2 = 1.9$
$C_3 = 0.7$
} core floating.

C. Testing Notes

The following points should be borne in mind when building and testing the discriminator.

1. As pointed out earlier in the paper, the larger the tunnel-diode output the higher the discriminator threshold must be set to avoid a relaxation oscillation. Since there is a range of output amplitudes among tunnel diodes, even of the same type number, they must be selected for low output if a sensitive discriminator is desired. The first indication of the threshold being set too low for a particular tunnel diode shows up in the discriminator's double-pulsing at a high input-signal level.

2. Improper selection of the bridge resistors R_1 and R_2 (Fig. 1) causes feedthrough. This appears as a step on the discriminator signal and may or may not be tolerable, depending of course on its size with respect to the tunnel-diode signal and the circuit that is to follow the discriminator.

3. Transformer (T_1) (Fig. 1) must be would rather carefully to avoid damaging the Teflon insulation. The techniques are described by the author in UCLRL Engineering Note EE 784 dated May 16, 1961.

FOOTNOTES

*This work was done under the auspices of the U. S. Atomic Energy Commission.

1. Yahia El Hakim, A Preliminary Investigation of the System Time Spread for Some Types of Multiplier Phototubes, Lawrence Radiation Laboratory Report UCRL-9200, May 11, 1960.

2. Proceedings of an International Conference on Instrumentation for High-Energy Physics, Berkeley, September 1960. (Interscience Publishers, New York, 1961).

3. Q. A. Kerns, A. E. Bjerke, and T. A. Nunamaker, Tunnel-Diode Discriminator Circuit, UCLRL Counting Group Note, September 7, 1960. (unpublished).

4. Q. A. Kerns, A. E. Bjerke, and B. E. Clark, Tunnel Diode Bridge Transformer-Type B, UCLRL Engineering Note EE-784, May 16, 1961.

5. One can take advantage of this width variation to obtain amplitude information by measuring the width of the direct tunnel-diode pulse; i.e., the unit is an inherent amplitude-to-time converter. A particular amplitude may be found by forming a delayed coincidence between the positive and negative differentiated pulses from the discriminator.

6. J. T Lavrischeff and S. Spataro, Evaluation of Deposited Carbon Resistors, Lawrence Radiation Laboratory Report UCID-961, December 10, 1959; J. T. Lavrischeff, Stock Proposal, Deposited Carbon Resistors, Lawrence Radiation Laboratory Report UCID-962, December 11, 1959.

7. These Multi-Tet ribbon cables are made of No. 22 copper wire insulated with 15-mil Teflon by W. L. Gore and Associates, Inc., Newark, Del.

FIGURE LEGENDS

Fig. 1. Tuned LC circuit diagram.

Fig. 2. Parts for 6810-A socket.

Fig. 3. The 6810-A socket assembly.

Fig. 4. The 6810-A assembled housings.

Fig. 5. Slewing characteristic of tuned LC circuit with 6810-A photomultiplier.

Fig. 6. Signal linearity.

Fig. 7. Output signal of 2N1143.

Fig. 8. Zero-crossing signals of 6810-A.

Fig. 9. Clipping-stub circuit diagram.

Fig. 10. Clipping-stub signal flow.

Fig. 11. Arbitrary clipping-stub input function.

Fig. 12. Effect of clipping-stub impedance on zero-crossing signal.

Fig. 13. Slewing characteristic of clipping-stub circuit with 7046 photomultiplier.

Fig. 14. Stability data for clipping-stub circuit. (a) Threshold changes over one-month period; (b) Threshold changes over two-month period.

Fig. 15. Installation of 100 clipping-stub circuits in a nuclear experiment.

Fig. 16. Clipping-stub circuit built as a plug-in unit.

Fig. 17. Equivalent circuit of tuned LC zero-crossing network.

Fig. 18. Generalized triangular input current pulse.

Fig. 19. Zero-crossing time for tuned LC circuit.

Fig. 20. Generalized triangular input current pulses to clipping-stub circuit.

Fig. 21. Zero-crossing time for clipping-stub circuit.

Fig. 22. Clipping-stub placed at base of photomultiplier.

Fig. 23. Sensitivity comparison of tuned LC and clipping-stub zero-crossing circuits.

Fig. 24. Bridge transformer.

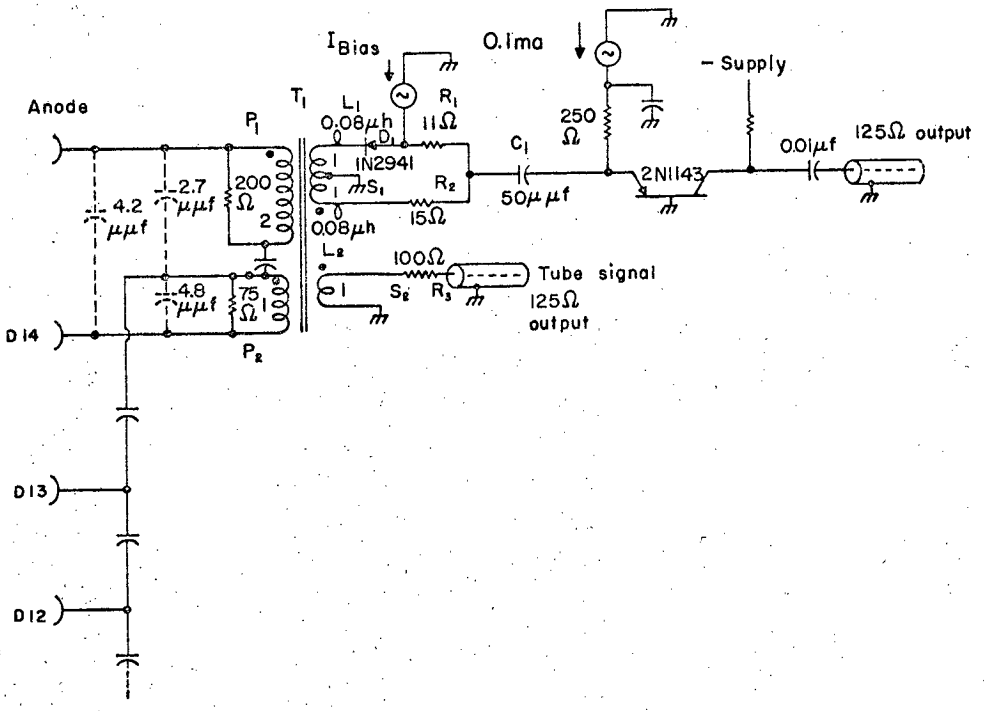
Anode
D14
D13
D12
4.2 μμf
2.7 μμf
200 Ω
2
4.8 μμf
75 Ω
1
P1
P2
T1
L1
0.08μh
D1
1N2941
S1
R1
11Ω
R2
15Ω
0.08μh
L2
100Ω
S2
R3
Tube signal
125Ω output
I Bias
0.1ma
250 Ω
C1
50μμf
2N1143
- Supply
0.01μf
125Ω output
MU-24748

Fig. 1.

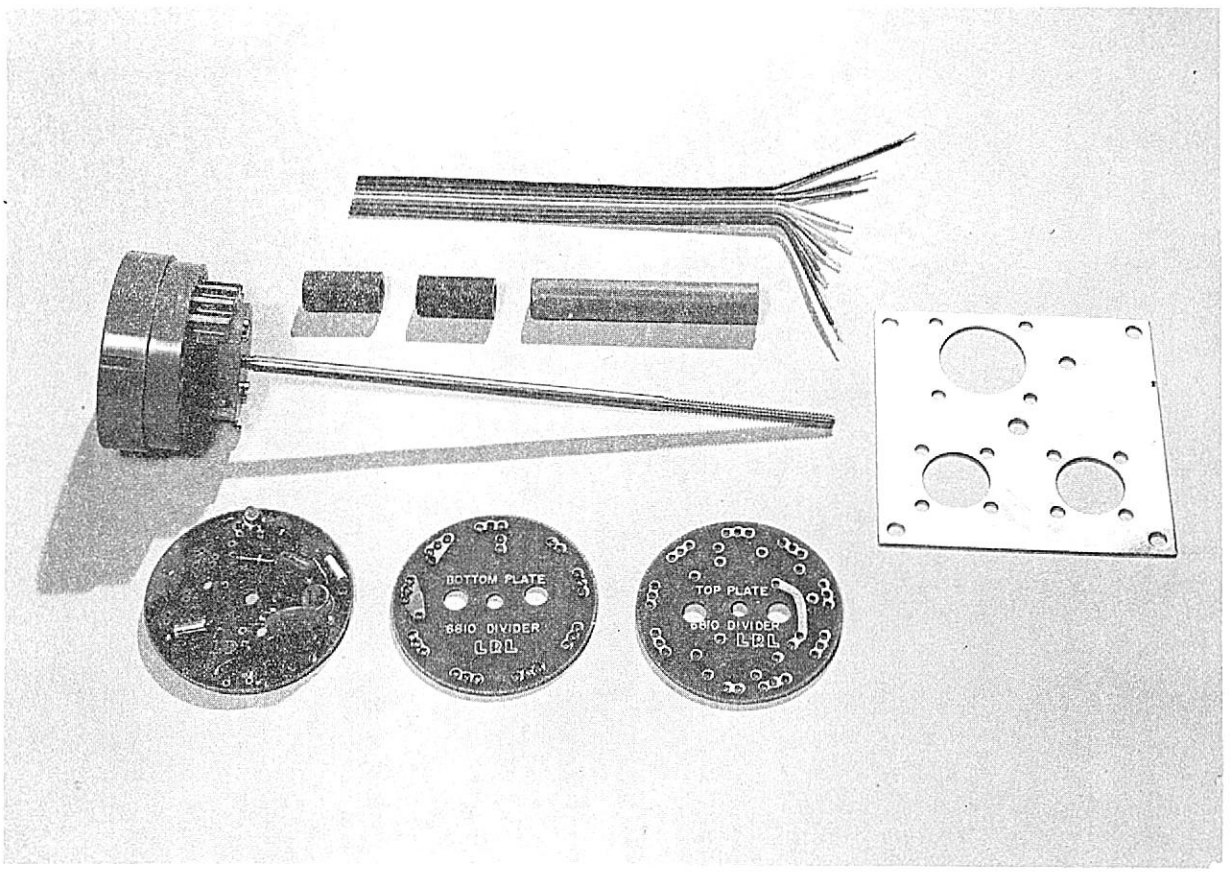

ZN-2902

Fig. 2

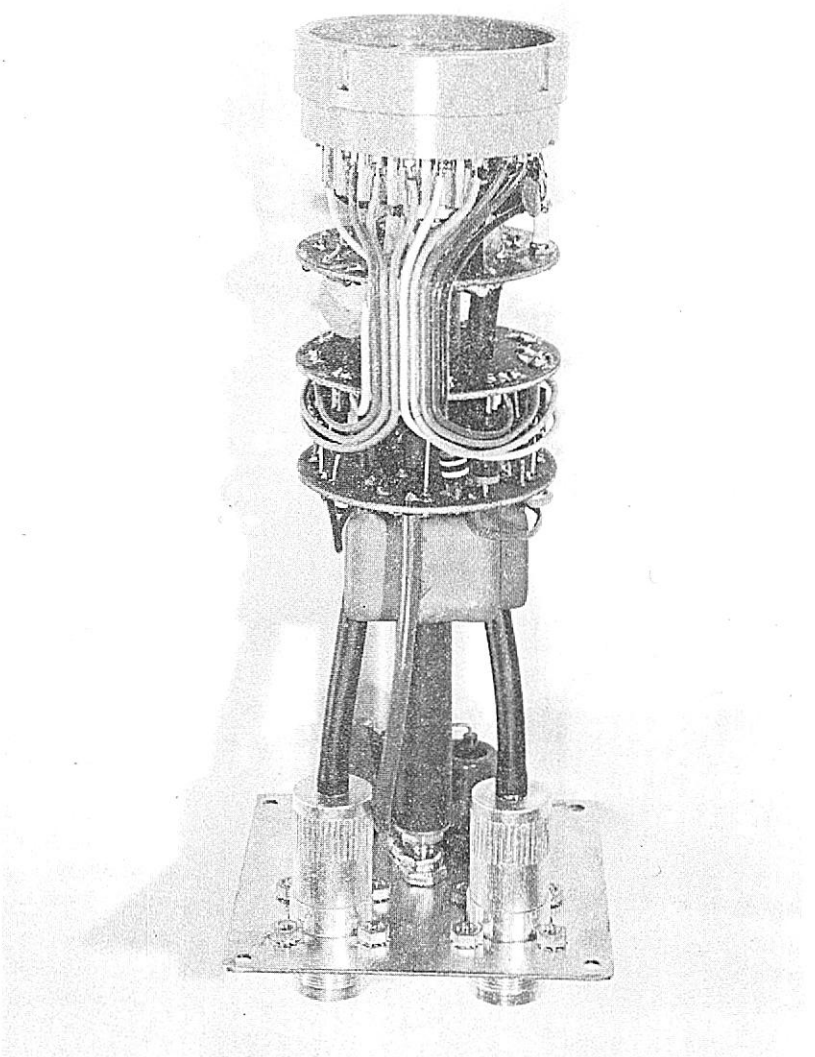

ZN-2906

Fig. 3

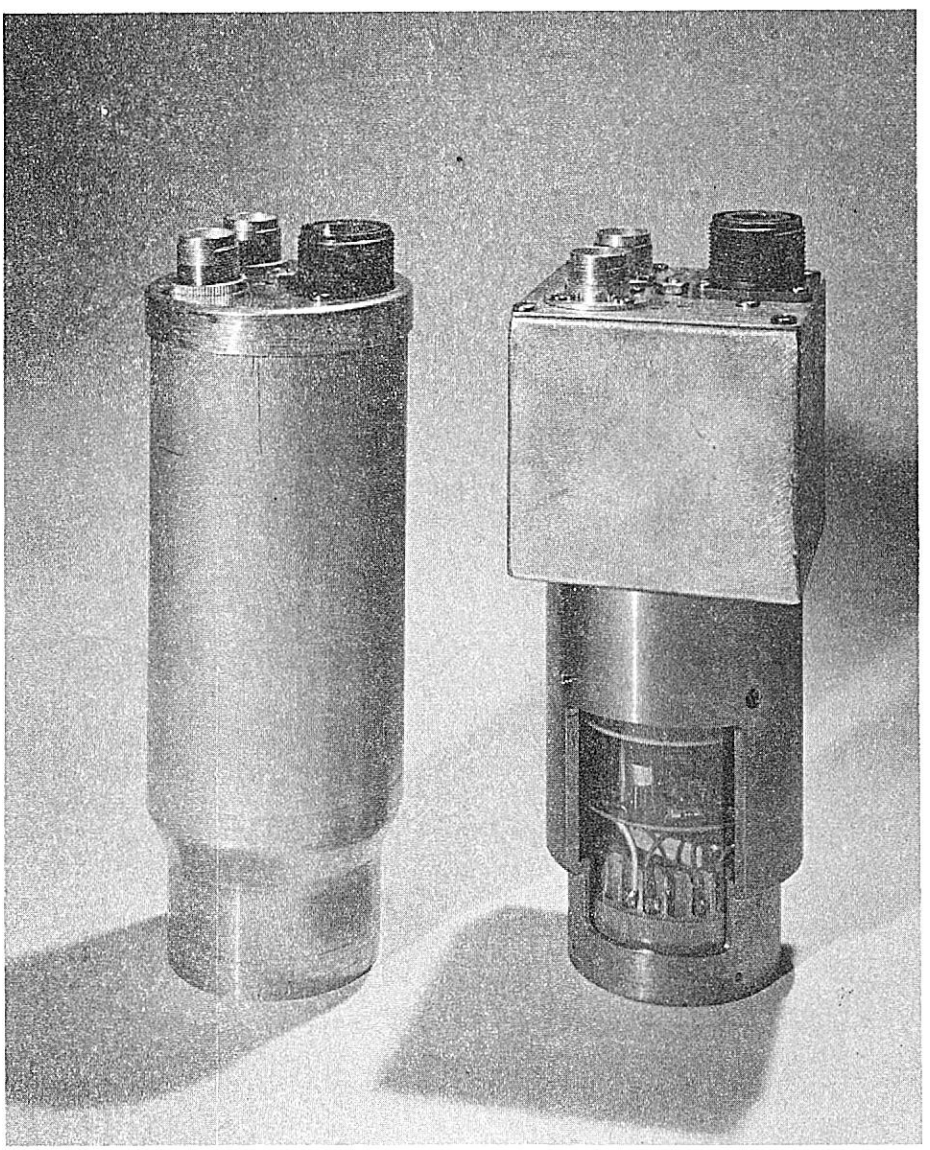

ZN-2904

Fig. 4

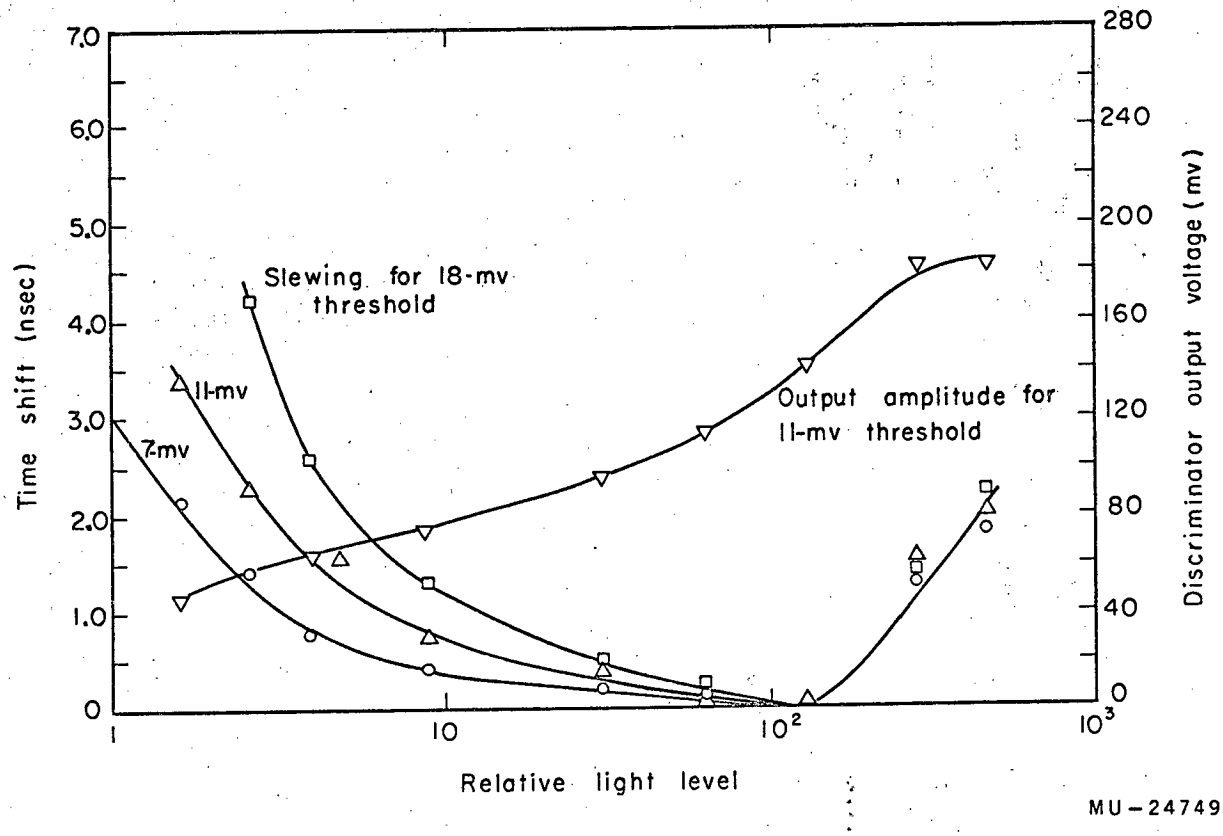
Time shift (nsec)
Discriminator output voltage (mv)
Relative light level
Slewing for 18-mv threshold
11-mv
7-mv
Output amplitude for 11-mv threshold
MU-24749

Fig. 5.

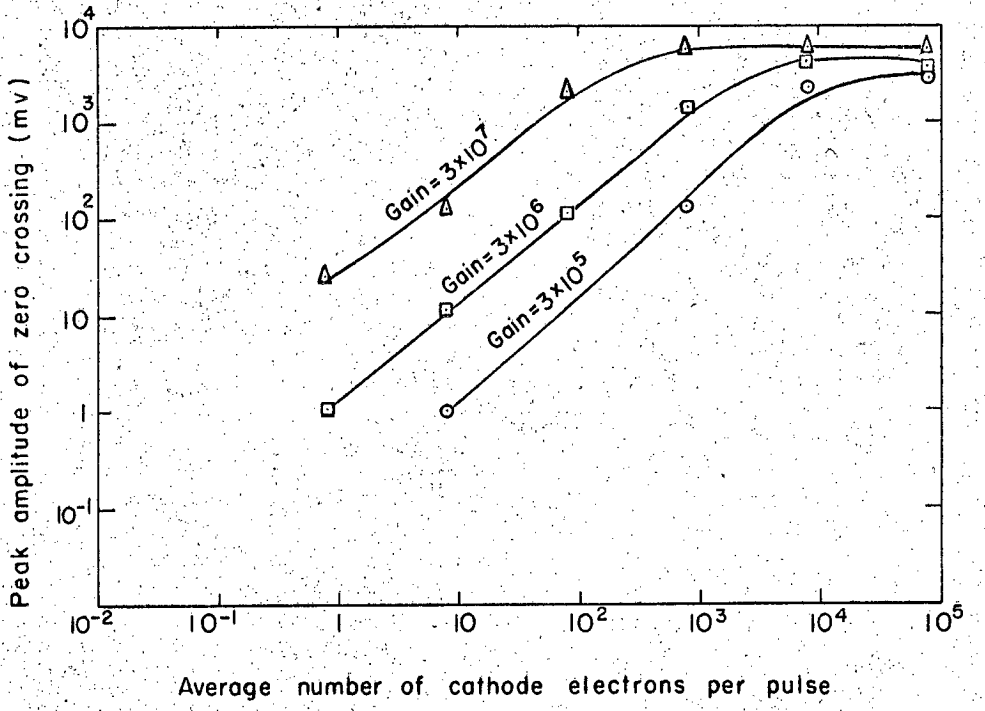
Peak amplitude of zero crossing (mv)
10^4
10^3
10^2
10
1
10^{-1}
10^{-2}
10^{-1}
1
10
10^2
10^3
10^4
10^5
Gain=3x10^7
Gain=3x10^6
Gain=3x10^5
Average number of cathode electrons per pulse
MU-24276

Fig. 6.

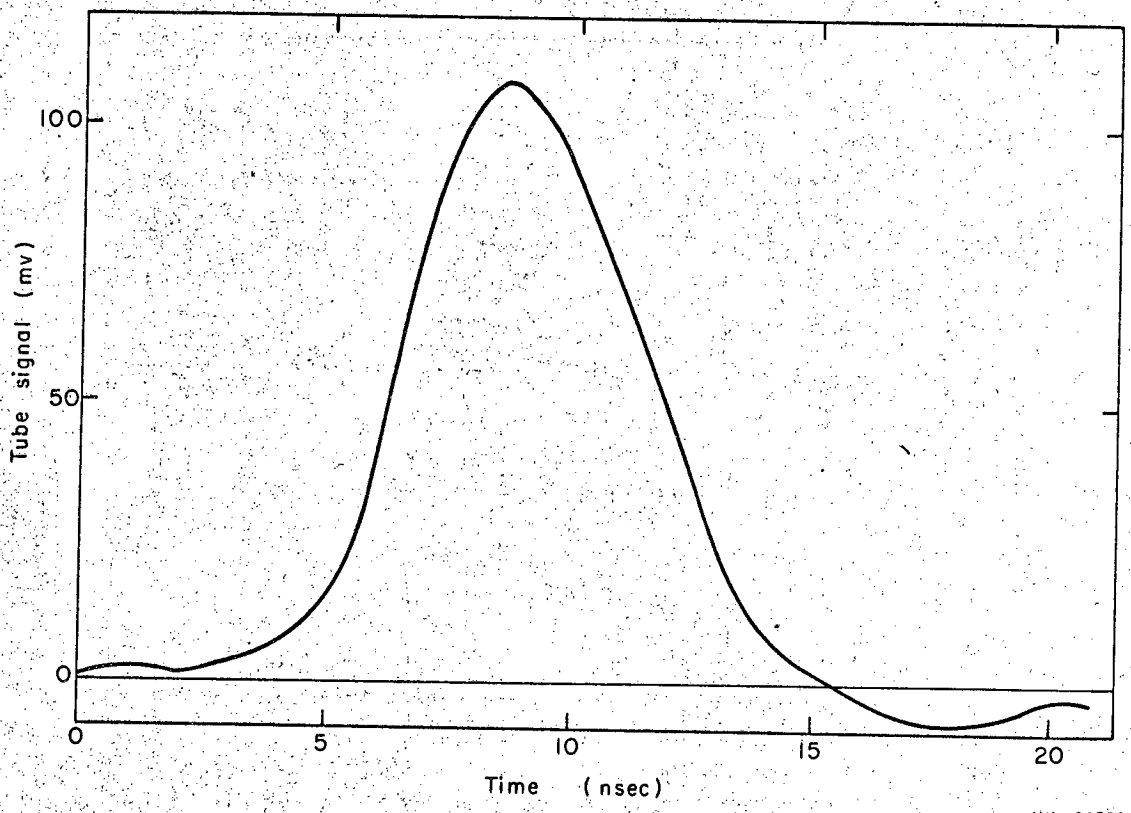

Fig. 7.

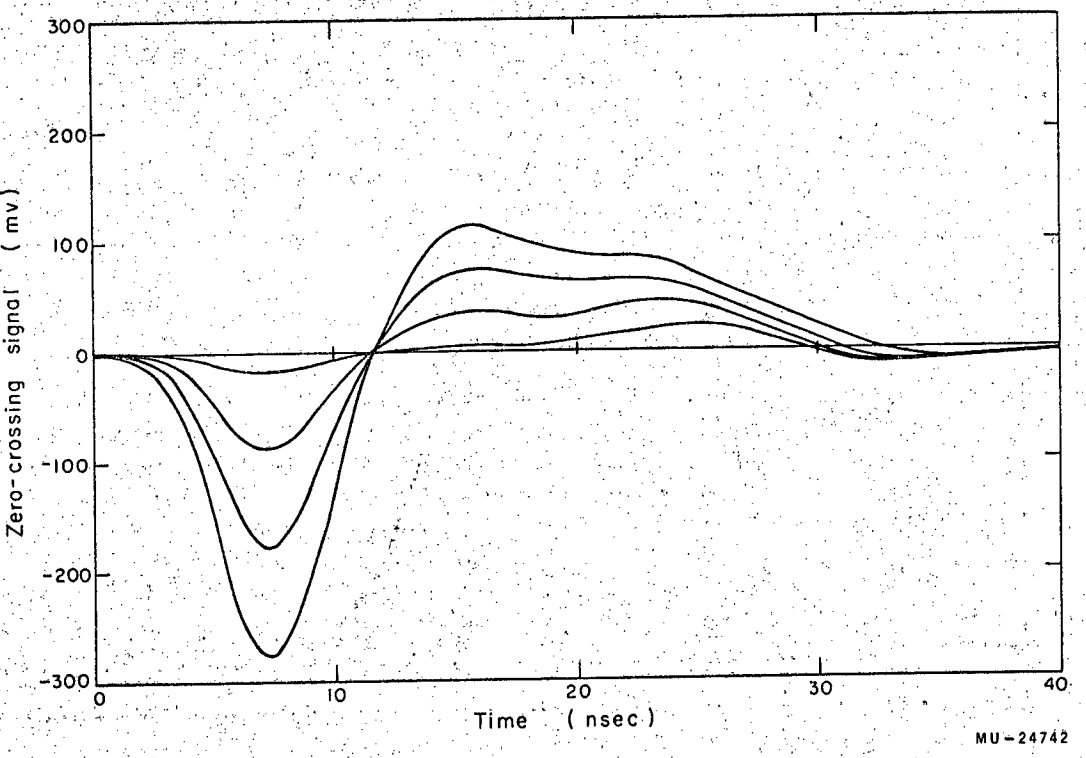
300
200
100
0
-100
-200
-300
0
10
20
30
40
Zero-crossing signal (mv)
Time (nsec)
MU-24742

Fig. 8.

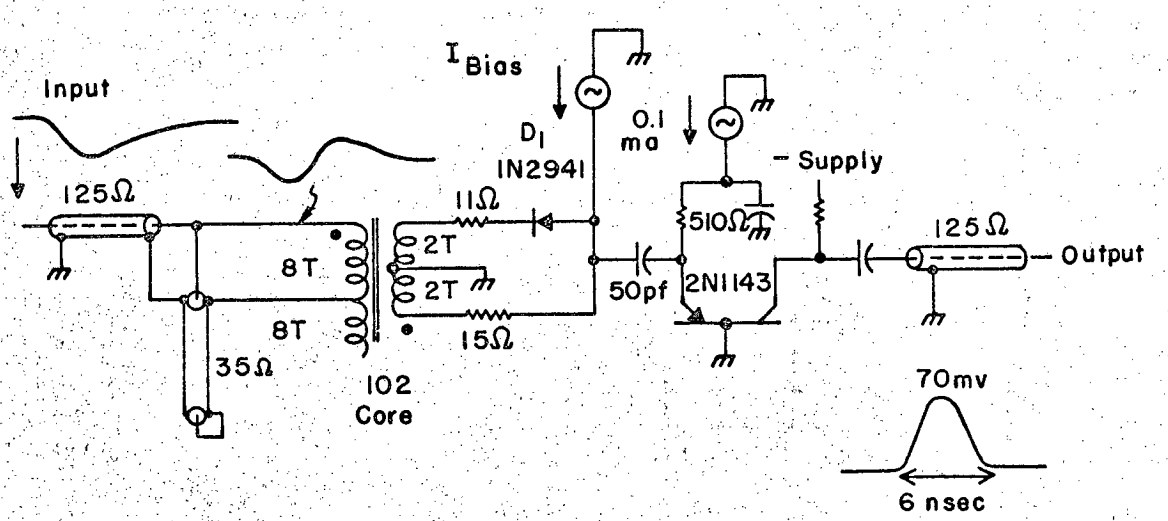
Input
125Ω
8T
8T
35Ω
102
Core
2T
2T
11Ω
15Ω
I Bias
D1
IN2941
0.1
ma
510Ω
50pf
2N1143
- Supply
125Ω
Output
70mv
6 nsec
MU-24743

Fig. 9.

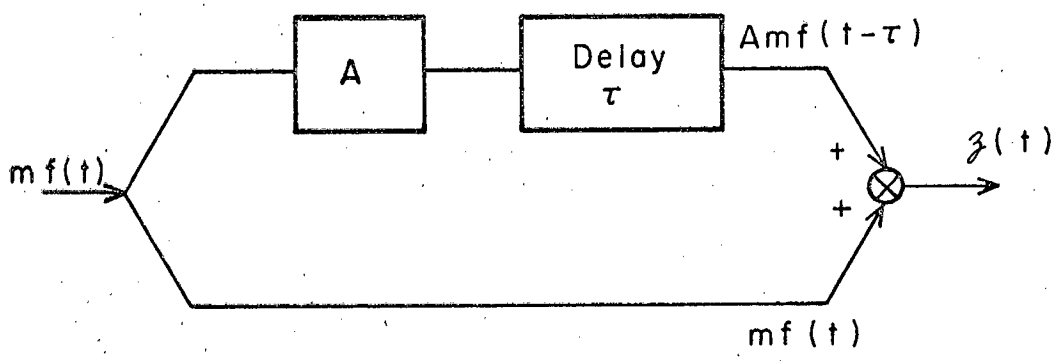

Fig. 10.

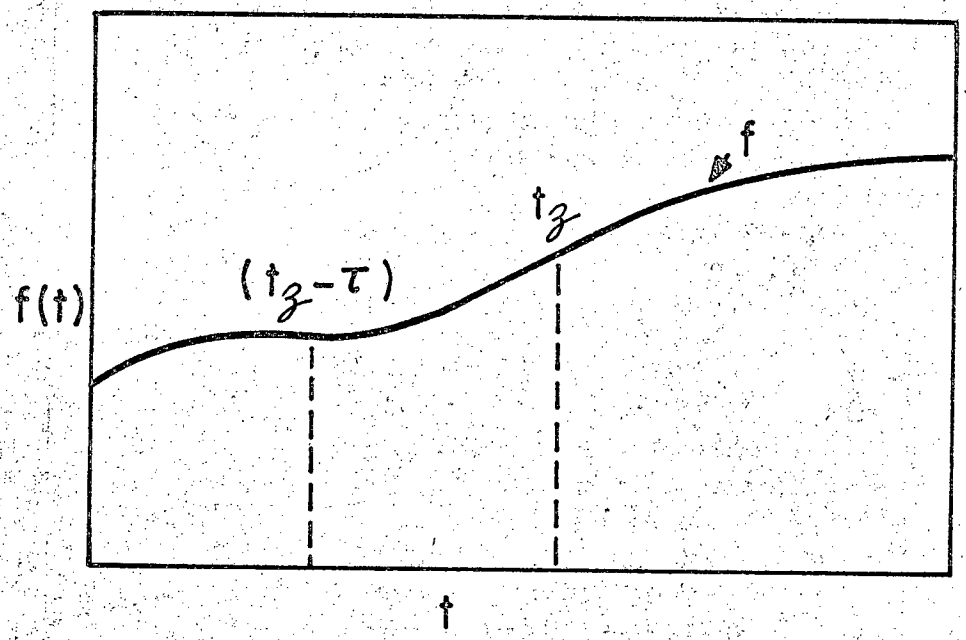

MU-25109

Fig. 11.

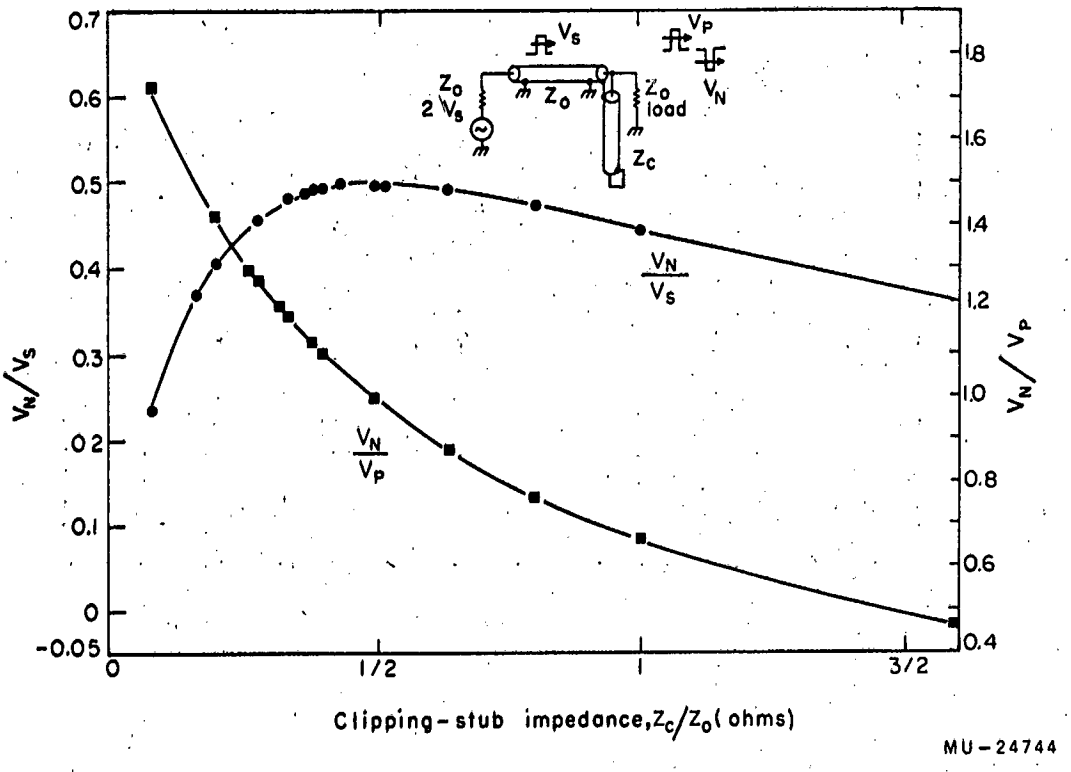
0.7
0.6
0.5
0.4
0.3
0.2
0.1
0
-0.05
1.8
1.6
1.4
1.2
1.0
0.8
0.6
0.4
0
1/2
1
3/2
V_N/V_S
V_N/V_P
$\frac{V_N}{V_S}$
$\frac{V_N}{V_P}$
V_S
V_P
V_N
Z_0
$2V_S$
Z_0
Z_0 load
Z_C
Clipping-stub impedance, Z_C/Z_0 (ohms)
MU-24744

Fig. 12.

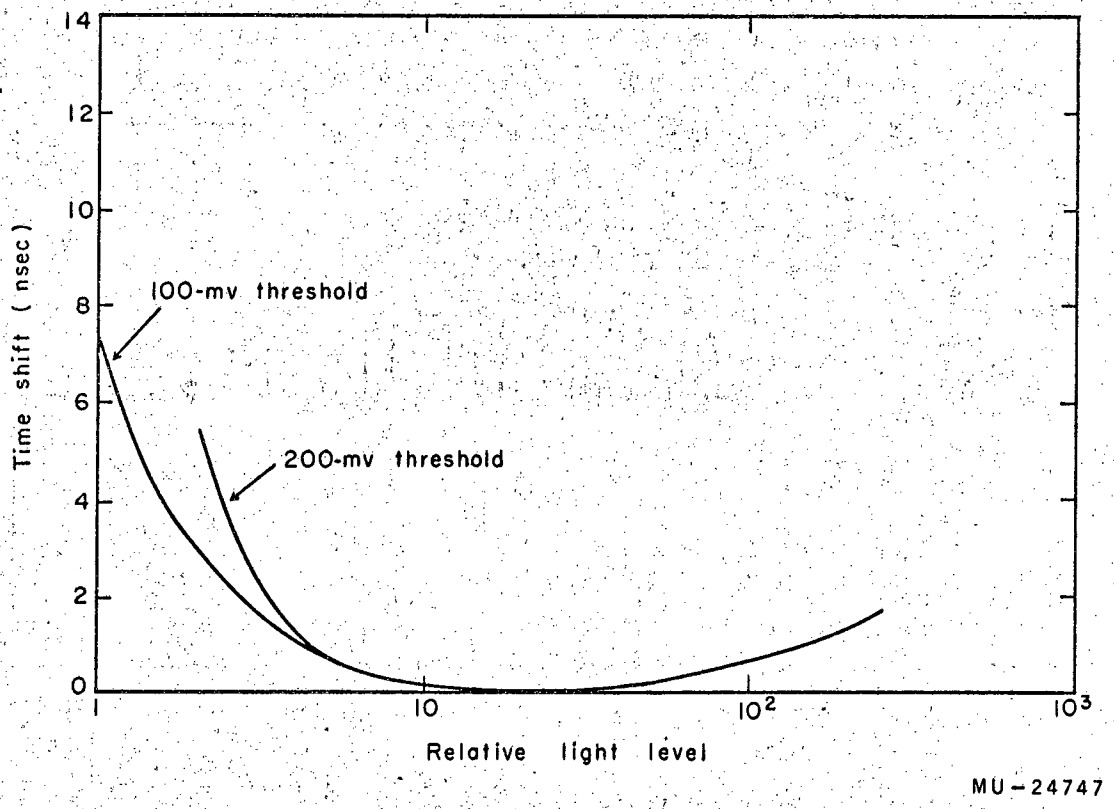
14
12
10
8
6
4
2
0
Time shift (nsec)
100-mv threshold
200-mv threshold
1
10
10²
10³
Relative light level
MU-24747

Fig. 13.

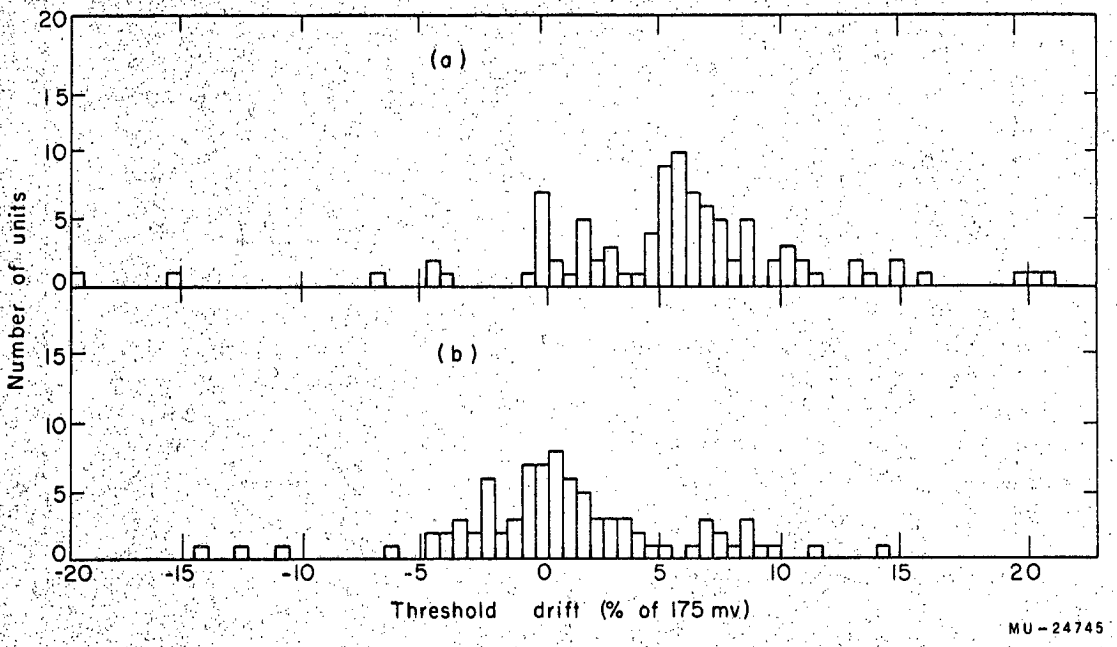
(a)
(b)
Number of units
20
15
10
5
0
-20
-15
-10
-5
0
5
10
15
20
Threshold drift (% of 175 mv)
MU-24745

Fig. 14.

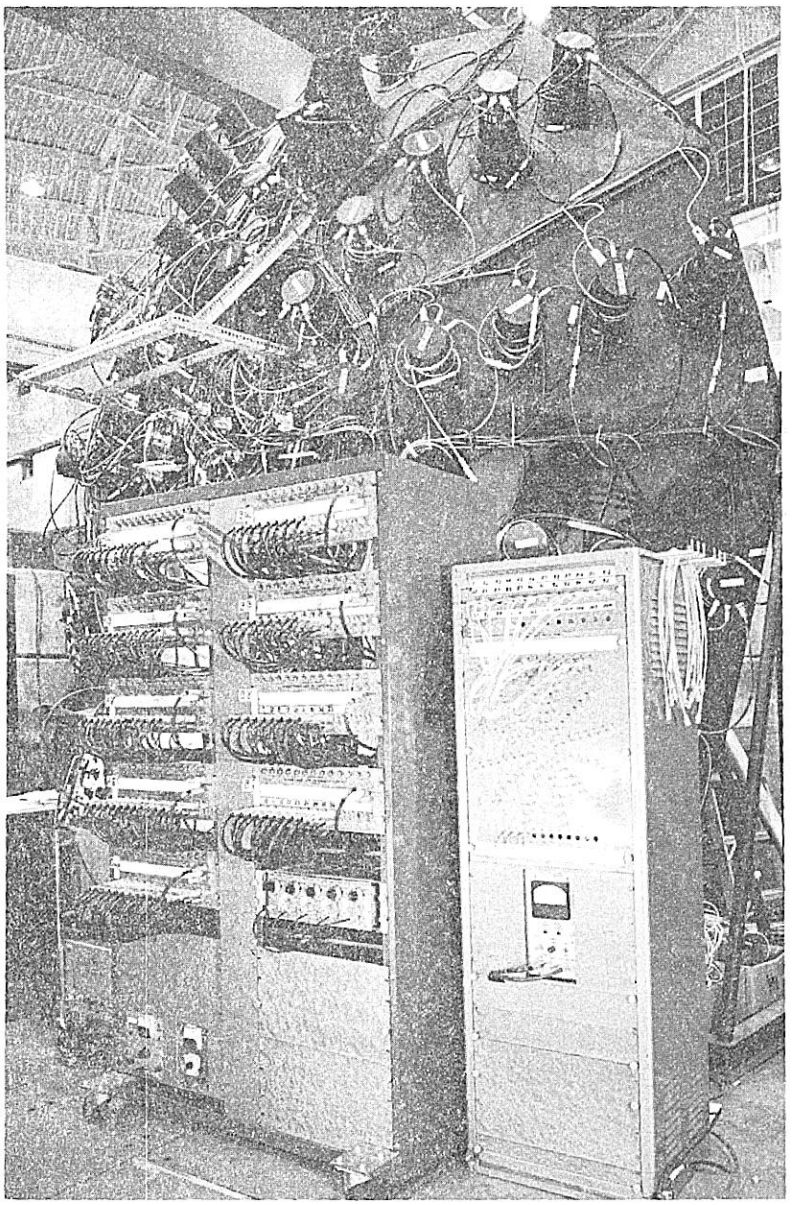

ZN-2903

Fig. 15

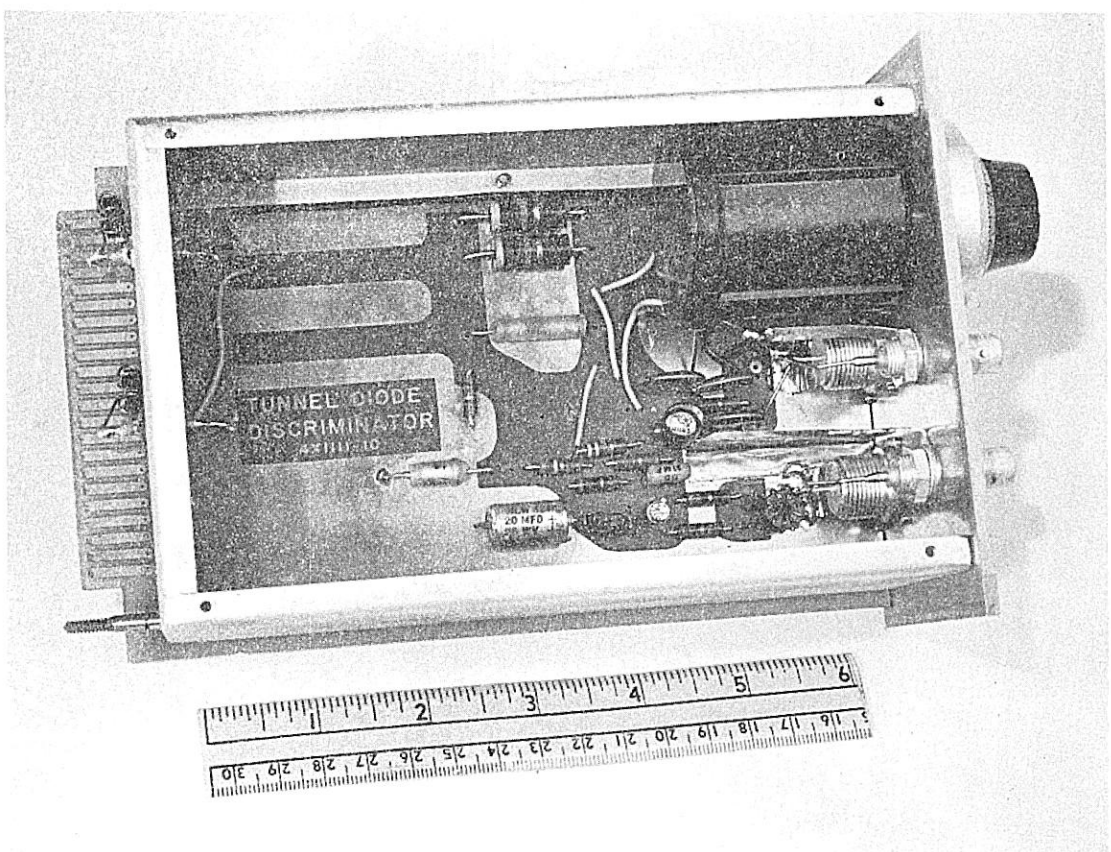

ZN-2905

Fig. 16

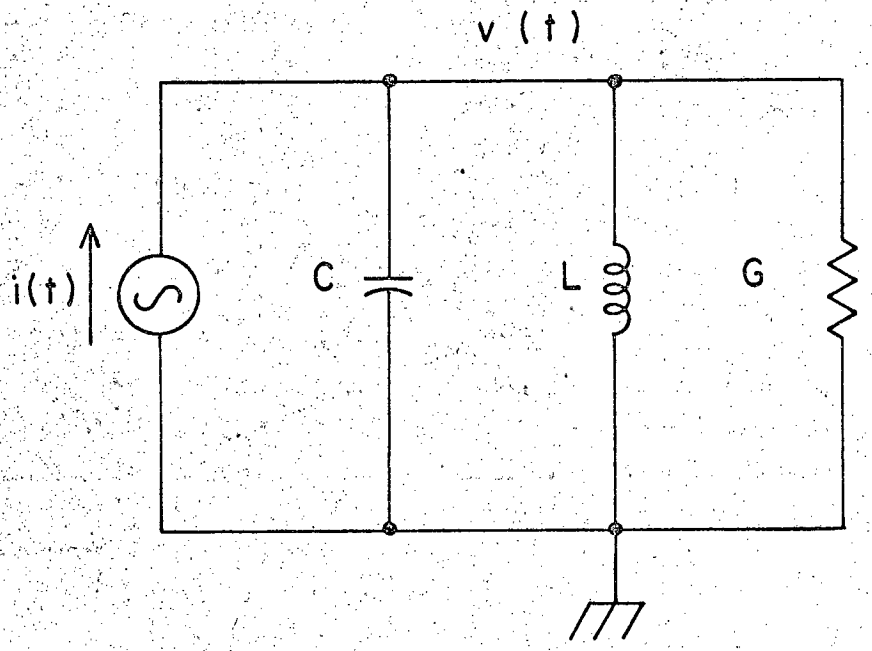

Fig. 17.

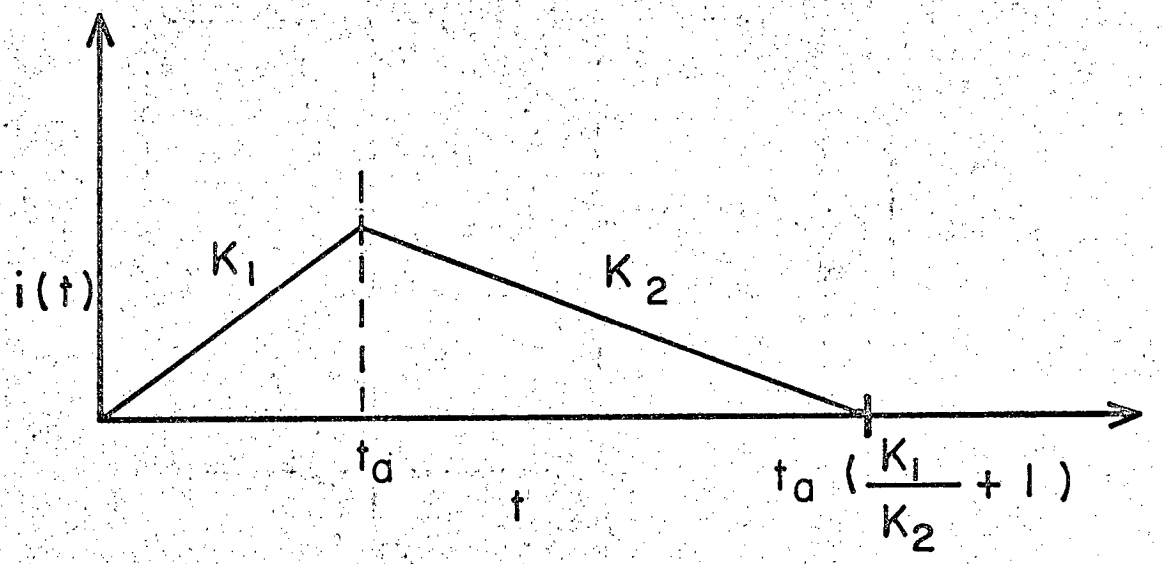

MU-25108

Fig. 18.

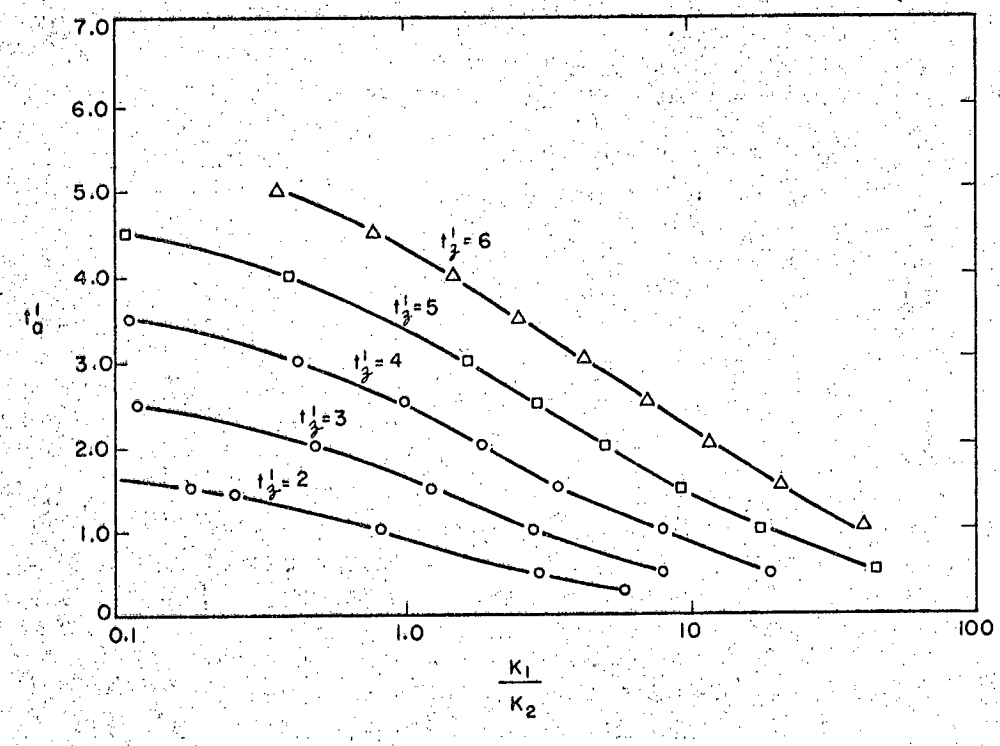
7.0
6.0
5.0
4.0
3.0
2.0
1.0
0
t'_0
$t'_{\frac{1}{2}}=6$
$t'_{\frac{1}{2}}=5$
$t'_{\frac{1}{2}}=4$
$t'_{\frac{1}{2}}=3$
$t'_{\frac{1}{2}}=2$
0.1
1.0
10
100
$\frac{K_1}{K_2}$
MU-25101

Fig. 19.

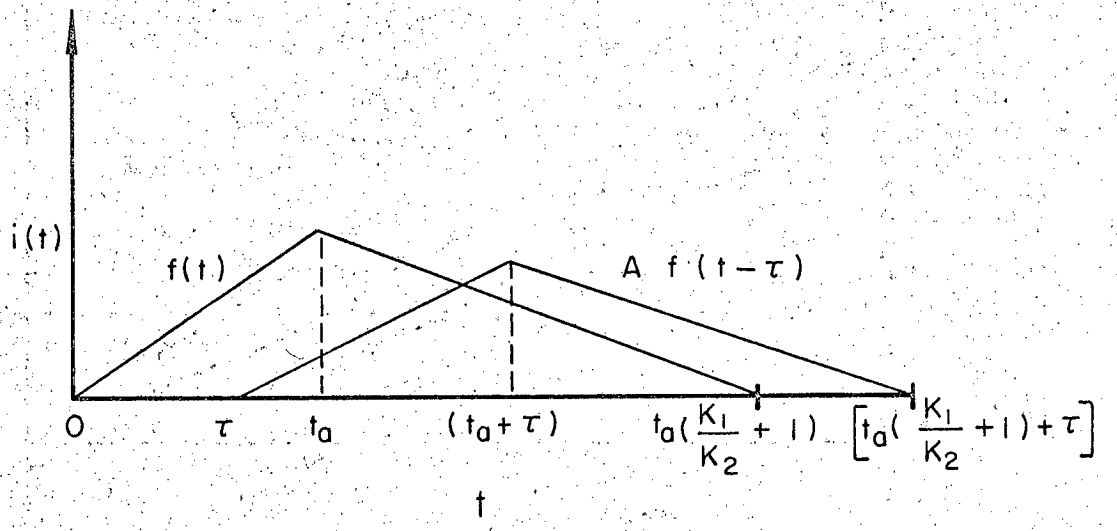

MU-25104

Fig. 20.

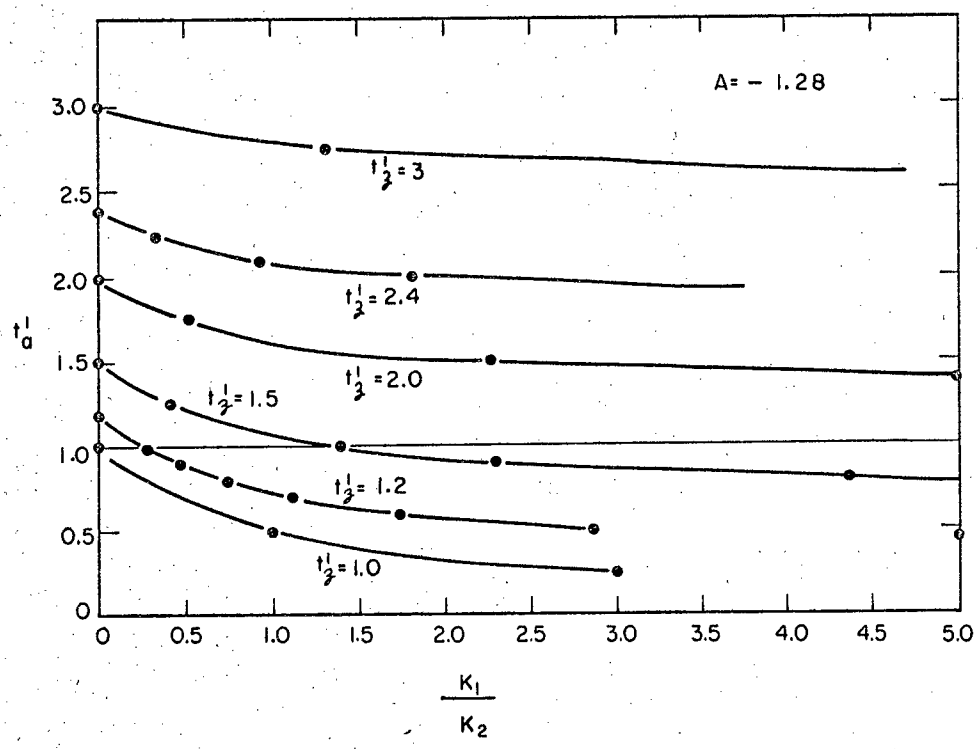
A= - 1.28
$t_{\frac{1}{2}}^{1}$ = 3
$t_{\frac{1}{2}}^{1}$ = 2.4
$t_{\frac{1}{2}}^{1}$ = 2.0
$t_{\frac{1}{2}}^{1}$ = 1.5
$t_{\frac{1}{2}}^{1}$ = 1.2
$t_{\frac{1}{2}}^{1}$ = 1.0
t_a^1
3.0
2.5
2.0
1.5
1.0
0.5
0
0
0.5
1.0
1.5
2.0
2.5
3.0
3.5
4.0
4.5
5.0
$\frac{K_1}{K_2}$
MU-25102

Fig. 21.

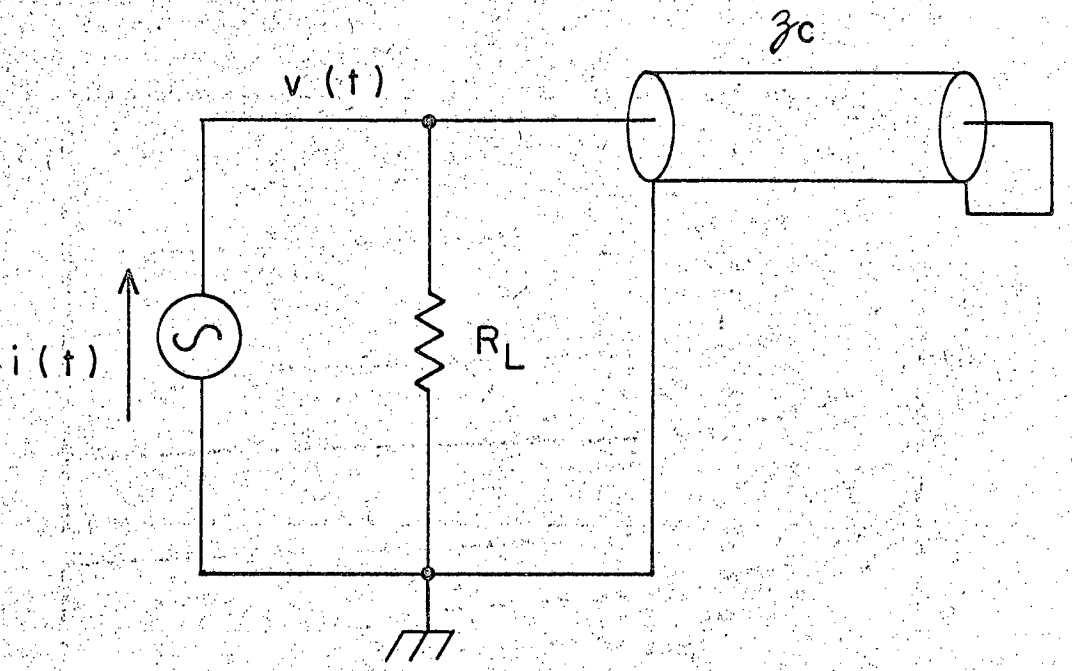

MU-25106

Fig. 22.

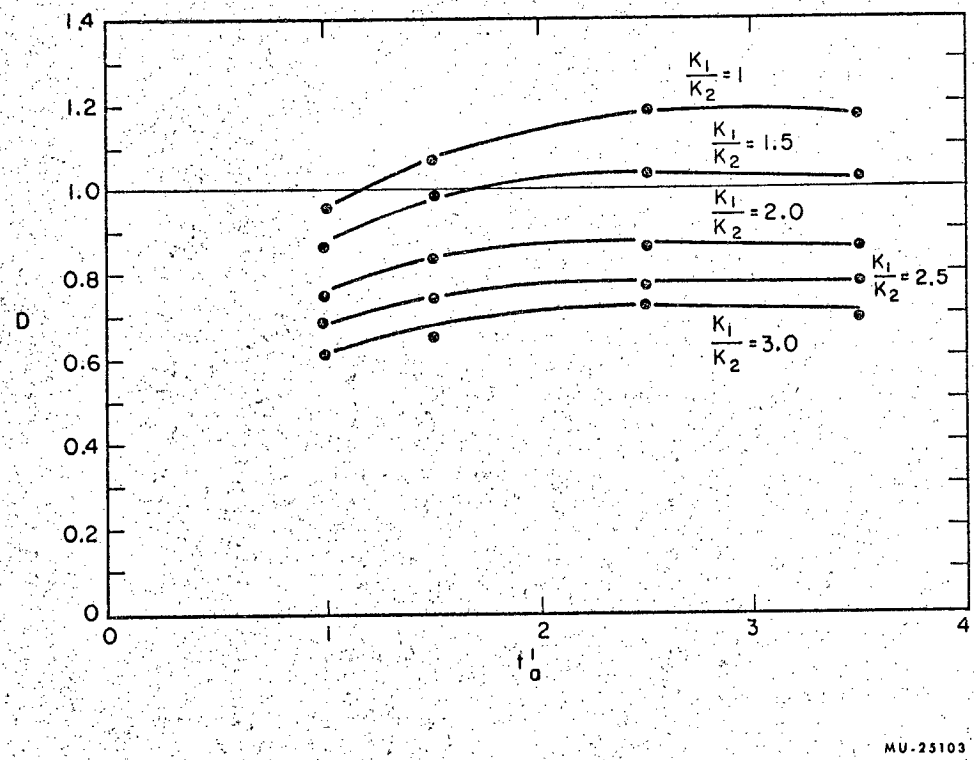
1.4
1.2
1.0
0.8
0.6
0.4
0.2
0
D
0
1
2
3
4
t'_a
$\frac{K_1}{K_2} = 1$
$\frac{K_1}{K_2} = 1.5$
$\frac{K_1}{K_2} = 2.0$
$\frac{K_1}{K_2} = 2.5$
$\frac{K_1}{K_2} = 3.0$
MU-25103

Fig. 23.

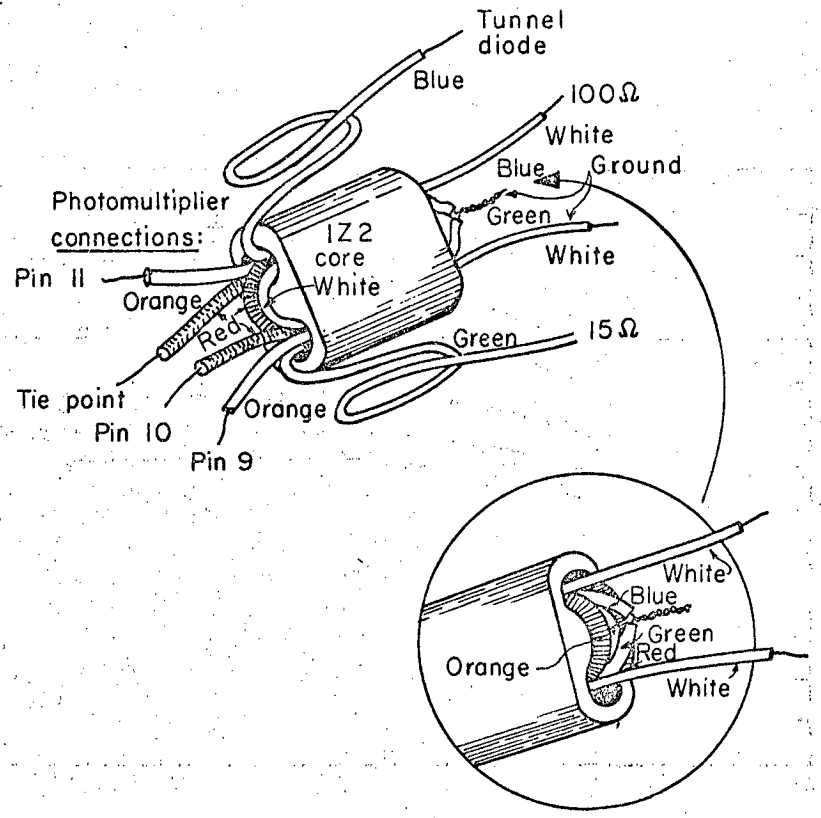
Tunnel diode
Blue
100Ω
White
Blue
Ground
Green
White
Photomultiplier connections:
Pin 11
Orange
Red
1Z2 core
White
Green
15Ω
Tie point
Pin 10
Orange
Pin 9
White
Blue
Green
Red
Orange
White
MU-24746

Fig. 24

This report was prepared as an account of Government sponsored work. Neither the United States, nor the Commission, nor any person acting on behalf of the Commission:

A. Makes any warranty or representation, expressed or implied, with respect to the accuracy, completeness, or usefulness of the information contained in this report, or that the use of any information, apparatus, method, or process disclosed in this report may not infringe privately owned rights; or

B. Assumes any liabilities with respect to the use of, or for damages resulting from the use of any information, apparatus, method, or process disclosed in this report.

As used in the above, "person acting on behalf of the Commission" includes any employee or contractor of the Commission, or employee of such contractor, to the extent that such employee or contractor of the Commission, or employee of such contractor prepares, disseminates, or provides access to, any information pursuant to his employment or contract with the Commission, or his employment with such contractor.